Polymer Bulletin (2022) 79:7065–7116
https://doi.org/10.1007/s00289-021-03899-0

REVIEW PAPER

Additive manufacturing: a review on mechanical properties of polyjet and FDM printed parts

Chandramohan Palanisamy[1,2] · Raghu Raman[2] · Pradeesh kumar Dhanraj[3]

Received: 11 June 2021 / Revised: 13 September 2021 / Accepted: 14 September 2021 /
Published online: 24 September 2021

Abstract

Additive manufacturing offers flexibility in designing, customizing, minimization of waste, manufacturing complex profiles and faster prototyping. Among these, polyjet and fused deposition modelling (FDM) process are widely employed to manufacture the parts for different applications. Hence, a comprehensive review on the mechanical properties of polyjet printed and FDM printed parts has been carried out in this paper. Under polyjet printing, influence of process parameters such as built orientation, built mode, finish type, part spacing and layer thickness on the mechanical properties has been discussed. Under FDM process, mechanical properties of important and potential polymeric materials such as acrylonitrile butadiene styrene, polylactic acid, polyether-ether-ketone and polyetherimide have been reviewed. Altogether, this paper gives an overview of mechanical properties of 3D printed parts, including a survey on selection of process parameters in polyjet process and materials selection in FDM process.

Keywords Additive manufacturing · Polyjet · Fused deposition modelling · Process parameters

✉ Chandramohan Palanisamy
pcmohu@yahoo.co.in

[1] School of Mining, Metallurgy and Chemical Engineering, University of Johannesburg, Johannesburg, South Africa

[2] Department of Mechanical Engineering, Sri Ramakrishna Engineering College, Coimbatore, Tamilnadu, India

[3] Scientist F, CEMILAC, Defence Research Development Organization, Bangalore, Karnataka, India

Introduction

AM attracts the interests of industry, research and academic sectors. Recently, cheaper and faster AM techniques that achieve great print quality have been created. In addition, polymer materials for 3D printing are now available with a broader range of qualities. These developments are constantly changing how items are created and made, as well as how people utilize them [1–4]. Because 3D printing considerably simplifies prototype creation, innovators and inventors may now easily build prototypes of their ideas. The design and manufacture processes have been simplified from weeks to a few hours [5]. AM has the potential to reduce manufacturing costs while also increasing overall efficiency. AM method is used to fabricate wide range of shapes and complex geometries from the three dimensional model data with short lead time [6]. The process involves printing layer by layer of materials to form a part [7]. Stereolithography (SLA) is the first and foremost method that was developed and subsequently other methods such as powder bed fusion (PBF), FDM [8], inkjet printing and contour crafting evolved [9]. Construction, fashion [10, 11], dentistry, medical [12–19], electronics [20], automotive [21], robotics, military, oceanography [22] and aerospace [23] are the applications for which AM is being actively investigated. Recent developments in 3D printing made its extension of applications such as in schools, homes, libraries and laboratories.

3D printing offers several advantages over the traditional techniques such as high precision, material saving, design flexibility and customization. A wide range of polymer processing 3D printing methods are existing; however, polyjet printing and FDM are being extensively employed in different applications. Large range of materials are being processed through the aforesaid 3D printing processes. Even then, the inferior mechanical properties of 3D printed parts still lower the potential of large-scale printing due to its anisotropic behaviour. 3D printed parts produced through these methods should be able to withstand a variety of mechanical and environmental pressures during their use in actual applications. It is crucial to understand the requisite strengths for each application under various loading circumstances, and 3D printed parts should, at the very least, have physical qualities similar to those produced by traditional processes [24–26]. This review paper focuses solely on mechanical characterization of polymer materials produced under polyjet and FDM in order to keep the scope as narrow as possible. Polymers are weaker than metals in general, but they have a lower density and larger strains at failure. Plastics have stronger strength per unit weight than metals in some circumstances. As a result of their reduced cost and flexibility to manufacture complicated designs, plastics may have greater advantages.

This review will compile the methodology followed for various types of mechanical testing and summarizes a vast amount of documented mechanical properties of 3D printed polymeric materials produced by polyjet and FDM techniques. Thereafter, focussed discussion will be provided on sample preparation (printing technique), polymeric materials with/without reinforcements, individual effect and combined of printing parameters, printers utilized, post-treatment,

testing machines, testing parameters, structure-property-parametric correlation, accuracy and cost aspect. Mechanical properties of polyjet and FDM printed polymers assessed in different conditions: tension, compression, bending, hardness, flexural, fatigue loading and impact loading will be discussed. The paper will be concluded with the key research results found from this extensive review which can serve as basis for future perspectives in enhancing the mechanical properties of the polyjet and FDM printed parts.

Mechanical properties of polyjet printed parts

Mechanical properties of the polyjet printed parts are greatly influenced by the parameters involved during built process as well as post-built. During processing, built orientation, built mode, finish type, part spacing and layer thickness are found to affect the properties of the parts. The effect of individual parameter as well as combined effect of different parameters on the properties of the polyjet printed parts is discussed in detail in the following sections.

Effect of print orientation on the mechanical properties of polyjet printed parts

Comparatively, a small number of engineering devices and structure are monolithic. Different combinations of materials are frequently required to meet the essential functionality and performance. Advancement in AM now allows multiple materials to be produced in a single manufacturing process, paving way for attainment of functional and performance targets. Interactions at the interfaces have been an interest in the area of adhesive bonding; similar issue requires to be addressed for printed composite materials including how print orientation and orientation of reinforcement may influence the properties or failure of the printed part [27]. Depending on the AM technology used, print orientation can have a substantial impact on the mechanical integrity of the finished product. Print orientation effects on modulus, strength and fatigue resistance have been proven in previous research [28–32], including for parts printed with various polymers [33, 34]. There are numerous studies that characterize the impact of print orientation on mechanical performance of the polyjet printed parts [35–38].

Table 1 summarizes the materials and their improved properties under the influence of print orientation. Ivan et al. [39] studied the influence of print orientation on interface integrity of photopolymers produced through polyjet printing (multi-material jetting) process. Acrylic-based two photopolymers such as TangoBlackPlus (TB) and VW Plus (VW) were printed using the Stratasys Objet350 Connex machine. Fracture resistance of the specimens consisting of layers of TB sandwiched between VW layers was tested using 5800R Instron (Canton, MA) at a cross head displacement rate of 1 mm/min. It was observed that fracture failure occurred at the material interface due to polymer fibrillation caused by surface imperfection or voids at the interface layer. It is concluded that the interface

Table 1 Summary of the materials and properties improvement under the influence of print orientation

Materials	Machine utilized	Variable parameters	Enhancement in properties	Ref
TangoBlackPlus (TB) and VW Plus (VW)	Stratasys Objet 350 Connex	Print orientation(X, Y and Z)	Better interface integrity with all orientation	[39]
VW Plus (VW) and RGD6	Stratasys Connex 3 Objet 500	Print orientation (X and Y)	Improved strength in X direction built specimen	[40]
RGD525	Connex 3D	Print orientation (X and Y)	Improved tensile and compressive strength in X direction built specimen	[41]
VW Plus RGD835	Objet260 Connex 3D	Print orientation (X and Y)	Improved tensile strength in X direction built specimen	[42]
Objet™Vero Grey™ and Digital ABS	Objet350Connex3™	Print orientation (X, Y and Z)	Improved bending strength and shore hardness in X direction built specimen	[43]
VW RGD83, High Temp RGD 525 and Clear Bio-compatible MED610	Connex 260	Print orientation (X, Y and Z)	Improved compressive strength in MED610 and VW RGD83 built in Z direction	[44]

integrity is found uniform with all the built orientation; hence, it is suggested for further deep understanding of deposition, consolidation and curing process.

Similar study has been carried out by Thomas Lumpe et al. [40] on investigating the tensile strength of multi-material interfaces fabricated through material jetting process using Stratasys Connex3 Objet500 3D printer. Tensile test specimens comprising two materials such as VW Plus and RGD6 were printed in matte finish option. Tensile tests were conducted according to the ASTM D638-14 standard using the Instron ElectroPuls E3000 testing machine containing Dynacell load cell of 5kN capacity and the obtained stress–strain curve is shown in Fig. 1.

Built specimen in X direction is found stronger than the Y direction built specimen which is attributed to the interfacial strength in multi-material specimens. In case of specimen built in X direction, the orientation of the inclusion increases the surface area of the interface, thus resulting in larger strength. In case of specimen built in Y direction, the inclusion was found larger compared to specimen built in X direction that makes the specimen weaker and induces failure at lower tensile load.

In addition to interface integrity, influence of the printing orientation on the mechanical properties has been studied. Rangarajan et al. [41] investigated the mechanical properties of objet high-temperature material (RGD525) manufactured through polyjet 3D printing under two different printing orientations (horizontal and vertical). Tensile specimens were printed according to the ASTM standard D638-10 and the tensile tests were carried out. Specimen built in horizontal direction exhibited tensile strength of 32.38 MPa and compression strength of 9.72 MPa. On the other hand, tensile specimens built in vertical direction possessed tensile strength of 27.52 MPa and compression strength

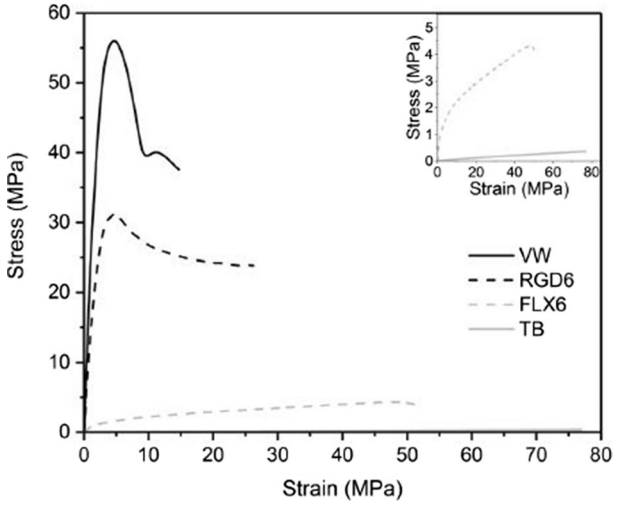

Fig. 1 Stress–strain curves of VW and RGD6 tensile test specimens (with kind permission from Elsevier publisher, [40])

of 8.88 MPa. It is concluded that horizontal built specimens exhibited greater strength in tension as well as in compression compared to vertical built specimens. It is understood that flat direction built parts have better quality than the vertical direction built parts.

Sai Charan Das et al. [42] investigated the effect of build orientation on tensile properties of polyjet 3D printed parts. Parts were printed using VW Plus RGD835 material and Full Cure 705 as the support material in six different built orientations using Objet260 Connex 3D printer. Parts were printed using the high speed mode and matte finish options. From the results, it is observed that Flat-X, Flat-45° and Vert-45° positions have better tensile strengths. Among all the specimens, Flat-X built has the highest UTS (58.57 MPa) with 8.19% increase compared to other specimens. This is attributed to the presence of cracks/voids in parallel to the direction of application of force in Flat-X built specimen. Thus, it will neutralize the effect of cracks, resulting in the high strength of the specimen. On the other hand, in vertical Y orientation, the cracks and voids are perpendicular to the direction of application of force which tends to magnify the effect of cracks resulting in lowest strength.

In addition to tensile strength properties, parts built in flat direction (X) even outperformed in bending and hardness properties. Peter Maroti et al. [43] produced Objet™Vero Grey™ and Digital ABS using the Objet350Connex3™ printer. Layer thickness maintained for ABS was 0.03 mm and for Vero Grey was 0.016 mm. Three-point bending test and shore D hardness tests were performed on the printed parts to assess its mechanical performance for implementation in prosthetic applications. Maximum bending stress of 62 MPa is resulted in ABS built in X direction, whereas bending stress of 60 MPa is attained in the Vero Grey built in X direction. It is concluded that building of prosthetics in X direction using these materials would benefit the special mechanical requirements. In case of shore hardness, Digital ABS built in X direction outperformed with the largest value of 76.6 ± 0.4. This is attributed to the continuous solid surface produced in ABS compared to that of the Vero Grey parts.

It is understood that special care should be taken in design as well printing processes, since properties of the printed parts are significantly influenced by the actual orientation of the printing. Hence, it is essential to consider all the orientation such as X, Y and Z orientation to study its influence on the properties. Therefore, Paul O Neill et al. [44] manufactured the parts via Polyjet inkjetting 3D printing technique using the Connex 260 from Stratasys. Parts were printed in three different direction (X, Y and Z) using three different polymer materials such as VW RGD83, High Temp RGD 525 and Clear Bio-compatible MED610. Compression tests were carried in the samples as per the ASTM D695 standard in Zwick/Roell Z050 UTM. Load cell of 50 kN is employed for performing the test at the cross head speed of 1.3 mm/min. Max compressive strength is resulted in MED610 part (95 MPa) and VW RGD83 (85 MPa) built in Z direction, whereas in High Temp RGD 525, maximum compressive strength of 50 (MPa) is attained in X direction built part. It is concluded from the study that MED610 part and VW RGD83 can be employed for making of embossing tools.

Combined effect of different parameters on the mechanical properties of polyjet printed parts

In AM process, build orientation has greater significance over the mechanical properties of the parts. Deliberation of all possible built orientations during printing process is highly essential. In addition, combined effect of build orientation, layer thickness, type of material, surface finish and post-processing plays significant role in mechanical properties of polyjet printed parts [45].

Table 2 summarizes the materials and their improved properties under the combined influence of different parameters. Aitor Cazon et al. [46] investigated the effect of printing orientation and post-treatment on the mechanical and surface properties of the Full cure 720 part produced through polyjet process. Eighteen different samples were produced under different printing orientation (xy, xz, yz, yz, zx and zy) using Objet Eden 330 printer. Parts were printed in three different finish such as glossy, matte (support material removed with water pressure) and matte (support material removed with water pressure + caustic soda). Tensile tests were performed on the specimens using Instron model 4467 machine under the head speed of 1 mm/min. Roughness tests were performed on the specimens using Mitutoyo SJ 301 portable roughness machine under the contact force of 0.75 N. Results reveal that specimens printed in X direction as major axis and glossy finish have greater resistance towards deformation with the ultimate tensile strength (UTS) of 42.20 MPa than the specimens printed in y or z direction. This is attributed to the action of load in longitudinal direction of the layers in parts build in X direction; hence, these parts tend to offer greater resistance to tensile load than Y and Z direction built samples. It is concluded that built orientation and finish process has greater significance over the final properties of the printed part.

In addition to build orientation, built mode also has significant influence with respect to surface finish type on the mechanical properties of the polyjet produced parts. Hence, Arivazhagan Pugalendhi et al. [47] investigated on the effect of process parameters such as built mode and surface finish type on the mechanical properties of VeroBlue made part produced under polyjet process. Specimens were produced using the Objet260 Connex printer in two different modes such as high quality (HQ) and high speed (HS) mode. Printed parts in two different modes (HQ and HS) were finished with matte and glossy types and classified as HQ-M, HS-M, HQ-G and HS-G. Tensile tests (ASTM D638) and flexural tests (ASTM D790) were performed on the specimen using Zwick Universal Testing Machine (UTM) for the speed of 50 mm/min. Shore hardness of the specimens was measured as per ASTM D2250 using shore D durometer at the temperature range of 68–70 °F. Tensile strength was found higher in HS-G specimen (49.47 MPa), whereas it was lower in case of HQ-M (47.4 MPa). HS-G specimen possesses the higher elongation of 34.33%, whereas the HQ-M yielded the lowest elongation of 26.66%. In case of flexural strength and shore hardness, HS-G specimen has performed better (25.83 MPa and 80.16 D) than all other combinations. It is concluded that part produced under HS-G mode has greater properties due to occurrence of perfect binding compared to HQ-mode. Therefore, this research work identifies that HS-G as a suitable combination for VeroBlue in polyjet process.

Table 2 Summary of the materials and properties improvement under the influence of combined effect of different parameters

Materials	Machine utilized	Variable parameters	Enhancement in properties	Ref
Full cure 720	Objet Eden 330	Print orientation (xy, xz, yz, yz, zx and zy) and surface finish type (glossy and matte)	Improved tensile strength in X direction built and glossy finished specimen	[46]
VeroBlue	Objet260 Connex	Built mode (HQ and HS) and surface finish type (glossy and matte)	Improved tensile strength elongation, flexural strength and shore hardness in HS-G specimen	[47]
VC and VW plus	Objet260 Connex	Built mode (HQ, HS and Digital) and surface finish type (glossy and matte)	Improved tensile strength, flexural strength and hardness in VC-G specimen	[48]
TangoBlackPlus	Connex 350	Built mode (Digital) and surface finish type (glossy and matte)	Improved fatigue life in glossy finished specimen	[50]
VC Fullcure 720	Stratasys EDEN 350 V	Local surface orientation (0, 30, 60 and 90°), layer thickness (16 µm and 30 µm) and finish type (glossy and matte)	Improved surface finish in specimen built under low layer thickness and glossy finish	[51]
RGD240	Stratasys Objet 30	Part spacing along X and Y axis (5 to 60 mm, orientation of part (0°, 15°, 30°, 45°, 60°, 75° and 90°) and surface finish (glossy and matte)	Improved modulus in specimens built closer to Y direction	[52]

The same research group studied the influence of process parameters such as built mode and surface finish on the mechanical properties of different materials such as VC and VW plus materials printed through polyjet process. Specimens were produced in Objet260 Connex printer in three different modes such as HQ, HS and Digital material (DM) mode. Parts under these modes were printed in matte as well as glossy finish and termed as matte finished VC specimens (VC-M), glossy finished VC specimens (VC-G), matte finished VW Plus specimens (VW-M) and glossy finished VW Plus specimens (VW-G). Tensile tests, flexural test and shore hardness tests were performed like in the previous study. The tensile strength and elongation obtained for the parts printed under different mode and finish are shown in Fig. 2. Tensile strength of the VC-G was found to be highest (53.6 MPa) and it is found lowest in VW-M (43.15 MPa); it was found to be the lowest. Average elongation of the VW-M is found higher (28.75%) followed by VC-G (24.5%), VW-G (23.5%) and VC-M (21.5%). Also, VC-G specimen has outperformed in flexural strength (49.1 MPa) as well as in hardness (81.37D). It is stated that VC-G specimens possessed superior mechanical properties than all other combinations. This is due to the minimal consumption of support material, faster printing time and glossy finishing. VC performed better than VW plus specimens due to its lesser printing time and material consumption [48].

In addition to the investigation on the tensile, flexural and shore hardness properties of the parts built under different mode and surface finish, fatigue properties of the parts also have to be investigated to fill a gap in the research. Traditional elastomers have the ability to experience large recurring strains without permanent deformation. Fatigue failure in the traditional elastomers occurs as the results of propagation of small tears present in the specimen owing to manufacturing. Voids and flaws generally caused by the layer-by-layer fabrication process may appreciably decrease the fatigue life of printed elastomers. Fatigue performance of the elastomeric-like materials was neither given by the manufacturer nor the research community. There is presently relatively little literature on the fatigue behaviour of additively manufactured polyjet parts, and further research is needed if these parts are to be employed in actual production [49]. Hence, Jacob et al. [50] investigated on the fatigue

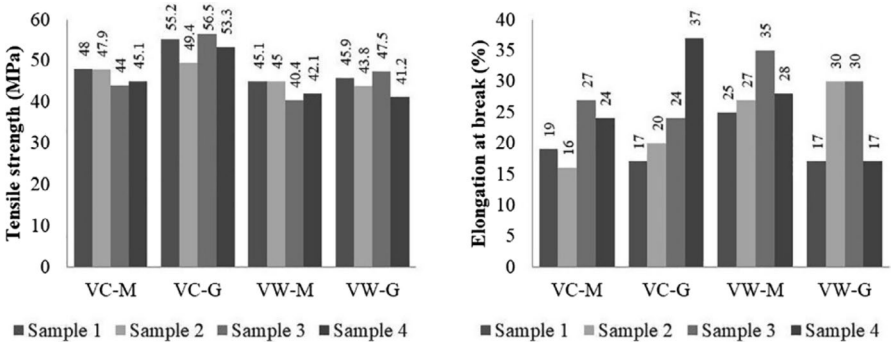

Fig. 2 Tensile strength and elongation of parts printed under different mode and finish (with kind permission from Elsevier publisher, [48])

performance of the TangoBlackPlus material printed through Connex 350 in "Digital Material" mode (i.e. 30 µm layer thickness) under two different finish (glossy and matte). Parts were printed with VW Plus (stiff) sections for the end and necks in the specimen, while the centre consisted of the TangoBlackPlus material. Fatigue tests were performed on the printed specimens in MTS Tytron250 Microforce Testing System with a 250 N load cell as per the ASTM D4482-11. Glossy specimen's possessed 37% increase in fatigue life compared to that of matte finished parts as this due to the glossy finished parts has approximately 20% lower surface roughness than the matte finished surface. Overall, it is concluded to avoid the part design that acts as local stress concentrators which have the tendency to shorten the fatigue life of the part.

As numerous parameters are involved in polyjet process, researches were focussed in studying the influence of combined effect on different parameters. This type of study brings out the optimal way of printing parts and attainment of exceptionally better mechanical properties through polyjet technologies. In such scenario, it is found that major factors that tend to affect the surface finish of the polyjet printed parts are layer thickness, local surface orientation and finish type. Surface finish of the polyjet parts has greater influence on extending its applications in several sectors. In addition, very few research works were oriented towards surface roughness investigation in polyjet parts. Hence, Krishnan Kumar and Gurunathan Saravana Kumar [51] investigated on the surface roughness of the photopolymer VC Fullcure 720 model material produced through polyjet process. Parts were printed in Stratasys EDEN 350 V machine with Fullcure 705 support material under the influence of process parameters such as local surface orientation (0, 30, 60 and 90°), layer thickness (16 µm and 30 µm) and finish type (glossy and matte). Printed samples were tested using the Mahr surf XR20 contact surface profilometer. It is observed that type of finish and local surface orientation has greater influence over the surface finish rather than the layer thickness. Increase in layer thickness increased the surface roughness marginally which is attributed to the staircase effect and this effect is very small for the range of layer thickness considered in process. Surface roughness found to increase as the local surface orientation increased from 0º to 90º due to the left over burrs on the surface by the support structures. It is concluded that model has been developed which enables the user to investigate the part build orientation and prefer the optimal orientation for attaining better surface finish in a polyjet printed part.

Similar kind of study was carried out by Gay et al. [52] on investigating the combined effect of different process parameters such as part spacing, orientation and surface finish on the mechanical properties of the polyjet printed RGD240 acrylic photopolymer parts. Parts were printed using the Stratasys Objet 30 machine with the gel-like photopolymer Fullcure 705 as the supporting material. Parts were printed with layer thickness of 28 µm and with common resolution of 42 µm (600 dpi). Four different parameters such as part spacing along X axis (5 to 60 mm), part spacing along Y axis (5 to 60 mm), orientation of part (0°, 15°, 30°, 45°, 60°, 75° and 90°) and surface finish (glossy and matte) are observed. RSA3 dynamic mechanical analyser (TA instruments) was used to evaluate the relaxation modulus E(t) by utilizing the three-point bending tool. It is concluded that part spacing in X axis and surface

finish do not have significant influence over the E(t). It is suggested to print parts in Y direction as closer as possible to have higher E (t). Regarding orientation, printing of part other than 45° direction has increased the properties of the material. Therefore, it is understood that fewer parametric condition has lesser/no significance over the properties, whereas fewer parametric condition has greater significance on the properties of the part.

Effect of post-treatment on the mechanical properties of polyjet printed parts

Mechanical properties of the polyjet printed parts are greatly dependant on the post-treatment processes such as heat treatment and high intensity ultraviolet (UV) curing. However, over-ageing upon heat treating of polyjet printed parts will tend to degrade the stiffness, ultimate tensile strength, strain at yield point and deformation [53]. Among these post-treatment process, high intensity UV radiation curing has high desirable capability to instantaneously harden the sprayed polymer. This curing tends to modify the physical and chemical properties of a material and specifically, for hardening or softening of a material. The length of UV exposure has a considerable impact on the mechanical characteristics [54].

Table 3 summarizes the materials and their improved properties under the influence of post-treatment.

Li Wang et al. [55] fabricated VC-RGD 810 parts through polyjet process using Objet Connex 3D printer. Specimens were printed upon different build-up orientation (S-X, S-Y and S-Z) and exposed to UV for curing. The SEM image of the UV-cured VC part is shown in Fig. 3.

Ultimate compressive strength of the parts was assessed using Digital servo-control UTM at the rate of 2 mm/min until failure. It is stated that part printed under all orientation behaved in a ductile manner. Average UCS of the S-Z is 3.7% higher than that of S-X and 4.4% higher than that of S-Y. The compressive strain–strain behaviour of the S-X, S-Y and S-Z samples is shown in Fig. 4.

Young's moduli (E) of the parts S-X, S-Y and S-Z are 2.21, 2.20 and 2.29 GPa, respectively. The higher mechanical performance of the S-Z samples is attributed to its construction height. Construction height of S-Z samples is found to be 10 mm, whereas the S-X and S-Y samples have the height of 5 mm. Construction height of the samples was found proportional to the UV exposure time. Higher exposure of UV in S-Z build samples has produced greater hardening effect which eventually improves the mechanical performance. It is concluded that post-treatment process can be carried out for significant enhancement of the mechanical properties.

Similar study on UV curing of materials was done by Sung Yong Hong et al. [56] on studying the mechanical properties and anisotropic behaviour of UV-curable 3D printed photopolymeric materials. Tensile specimens of five different thickness 0.5, 0.8, 1.0, 3.0 and 5.0 mm were printed using Objet350 Connex polyjet type 3D printer according to the standard ASTM D638. Uniaxial tensile tests were carried out using the Instron ElectroPuls E3000 (Instron Ltd, High Wycombe, UK) at the rate of 1 mm/min with 3kN load cell. It is observed that specimens with 5 mm thickness exhibited greater tensile strength of 32 MPa among all the specimens which

Table 3 Summary of the materials and properties improvement under the influence post-treatment

Materials	Machine utilized	Variable parameters	Post-treatment	Enhancement in properties	Ref
VC-RGD 810	Objet Connex 3D	Built orientation (S-X, S-Y and S-Z)	UV curing	Improved compressive strength and Young's moduli in S-Z built specimen	[55]
3D printable UV-curable resin	Objet350 Connex	Different thickness (0.5, 0.8, 1.0, 3.0 and 5.0 mm)	UV curing	Improved tensile strength in higher thickness specimen	[56]
VW Fullcure 830	Stratasys EDEN 260 V	Sheet thickness (17 µm)	UV curing	Improved tensile strength in cryogenic environment	[57]
Dental long-term (LT) resin	Formlabs 3D	0.75 mm thickness	UV curing	Improved compressive strength in specimens cured for longer time	[69]

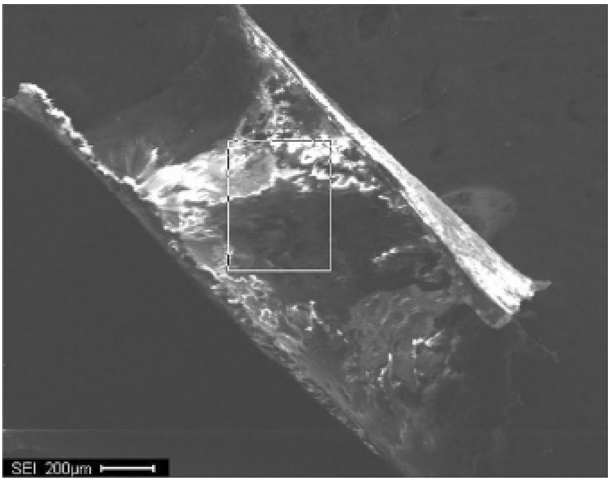

Fig. 3 SEM image of UV-cured VC (With kind permission from Nature publisher [55])

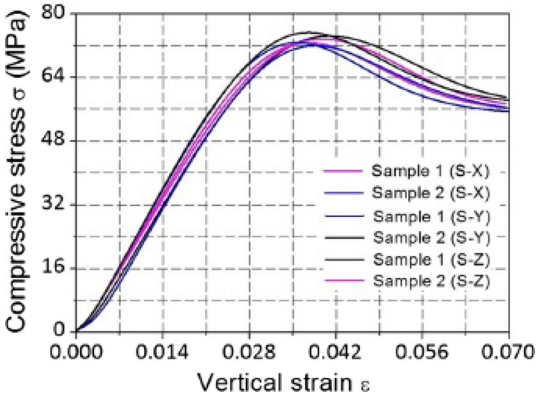

Fig. 4 Stress–strain curves of 3D printed S-X, S-Y and S-Z samples under uniaxial compressive conditions (with kind permission from Nature publisher [55])

is evident that the tensile strength gets increased with increase in thickness of the specimen, as shown in Fig. 5.

This is due to the nature of the polyjet printing technique which builds in a layer-by-layer stacking process. For thicker specimens on printing subsequent layers, extra UV-light exposure to the previously printed layers has promoted further polymerization of residual unreacted monomers and eventually improves the mechanical properties. It is concluded that such UV-light exposure tends to enhance the properties as closer to the epoxy polymers commonly used and enhances its usage in a wide variety of engineering applications.

On the other hand, AM thermoplastics are so far not often considered for cryogenic applications but are potential alternative for complex cryogenic parts and constructions. Rare data on properties of the AM parts on this low temperature regime were available. Therefore, Weiss et al. [57] have investigated on the mechanical strength of VW Fullcure 830 to evaluate their application in the cryogenic

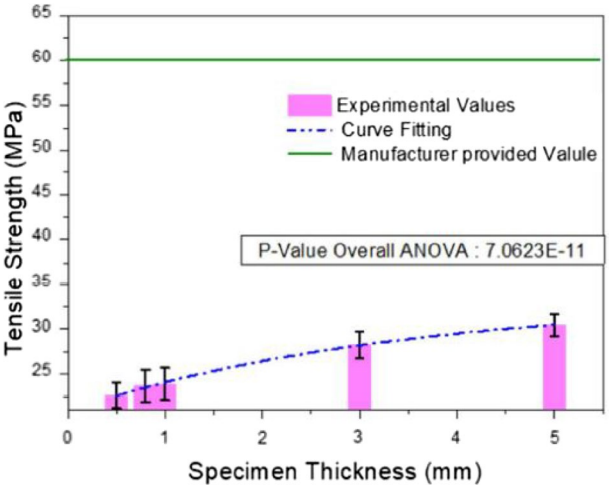

Fig. 5 Size-dependent tensile properties of UV-curable 3D printed photopolymeric material (with kind permission from Elsevier publisher [56])

temperature environment. Specimens were printed using polyjet modelling in Stratasys EDEN 260 V device with sheet thickness of ~ 17 µm. The temperature of the system was maintained ~ 50–60 °C, and the curing was done by UV radiation. Tensile test specimens were printed according to the DIN EN ISO 527–2. Tests were performed at room temperature of about 293 K (RT), liquid nitrogen temperature (77 K) and immersed in liquid helium (4.2 K) and UTS of 36, 46 and 32 MPa was resulted, respectively, as observed in Fig. 6. It is suggested that developed specimen having better strength would be a better alternative for using in liquid nitrogen exposed conditions.

Apart from normal temperature and cryogenic applications, medical industry was found to have more usage of the polyjet printed parts in the recent days [58, 59]. In specific, dental aligners were providing a long-term treatment process for aligning misaligned teeth of patients for their perfect aesthetic smile, since 75% of the adult

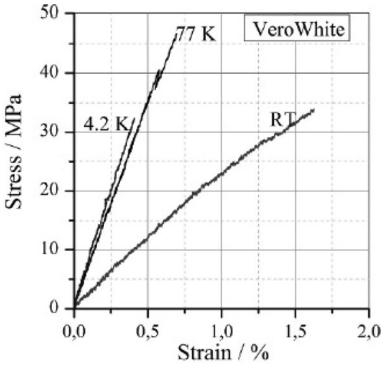

Fig. 6 Stress–strain curve of VW Fullcure 830 with different temperatures such as 293 K (RT), liquid nitrogen (77 K) and liquid helium (4.2 K) (with kind permission from IOP Publisher [57])

patients are found unsatisfied with their dental appearance [60]. Hazeveld et al. [61] introduce the AM technique as the method for fabrication of dental plaster models and stated that AM manufactured plaster models can be suitable alternative for the conventional plaster models. El Katatny et al. [62] attempted fabricating of dental plaster models for different humans sizes and gender. Geometric accuracies are found higher with AM manufactured dental plaster models [63]. It is reported by several researchers that AM-made dental aligners are found mechanically strong and bio-compatible [64–68]. Therefore, Prashant Jindal et al. [69] studied the compressive mechanical properties of polyjet printed dental long-term (LT) resin-based clear aligners. Aligners were designed and printed to 0.75 mm thickness using Dental LT resin as shown in Fig. 7.

Curing process was carried out at 80 ºC for different time of 15 and 20 min, and its performance was compared with the uncured specimens. Compression testing on the aligners was conducted through the Instron 3367 UTM under the load of 1000 N at the rate of 50 N/min. Uncured aligners withstand a lower load of 380 N due to severe plastic flow and higher deformation. On the other hand, aligners cured at 80 ºC for 20 min withstand maximum compressive load of 662 N compared to the sample cured for 15 min (531 N). The load–displacement curve for the different samples is shown in Fig. 8.

This is attributed to the brittle transformation of the material upon curing which tends to resist the compressive deformation. It is concluded that these experimental investigation provided a clear insight towards designing and printing of dental aligners with adequate mechanical strength.

Elastic modulus of the polyjet printed parts

In the field of tissue engineering, the ability to produce sophisticated porous structures at a fraction of the expense of traditional manufacturing methods has made

Fig. 7 Polyjet printed dental long-term (LT) resin-based clear aligners (with kind permission from Elsevier publisher [69])

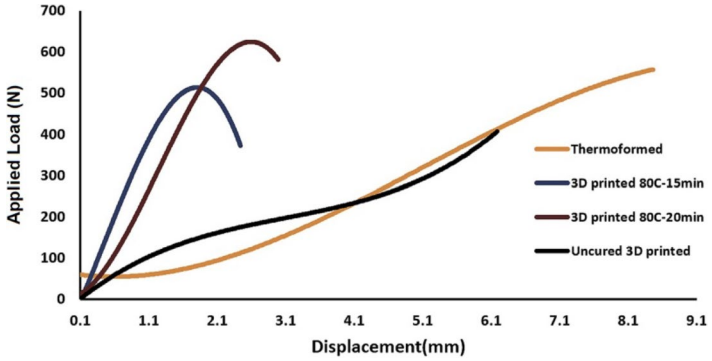

Fig. 8 Compression behaviour of the cured and uncured aligners (with kind permission from Elsevier publisher [69])

3DP the favoured alternative for scaffold fabrication [70]. In recent years, micro-scale scaffolds for bone replacement and regeneration, in particular, are of tremendous interest [71–74]. Bone scaffolds temporarily replace the defected or lost bone section until the regeneration process is taken place and new bone tissue is produced [75–78]. The mechanical properties of scaffolds used for bone regeneration play an important role in determining the possibility and quality of cell regrowth and proliferation [79]. One of the important considerations during manufacturing of the scaffolds in terms of their mechanical properties is the elastic modulus specifically while development of the cancellous structure such as trabecular bone. Table 4 summarizes the materials and the improved elastic modulus of polyjet printed parts.

Morteza Amini et al. [80] fabricated VW Plus part with water-soluble SUP707 and normal SUP705 support materials using Stratasys Polyjet (OBJET EDEN 260VS™) 3D printer. Parts were printed under two different resolutions (16 and 32 μm). Tensile tests were performed on the printed part as per the ASTM 638 standard. Higher resolution found to increase E modulus and strength by 23% and 12% than that of the lower resolution printed parts.

Similarly, Paul Egan et al. [81] fabricated lattice samples in Stratasys Objet500 Connex3 printer using MED610 bio-compatible polymer and SUP706 support material. Polymer lattices were developed with 50% and 70% porosity with the beam diameters of 0.4–1.0 mm. Mechanical properties were assessed using quasi-static compression with an Instron E10000 ElectroPuls. Elastic moduli of the printed parts are ranging from 8 to 213 MPa, and it is found decreased with increase in the lattice porosity and increased with larger beam diameters. Stiffness of the printed parts ranged between 4.1 kN/mm and 9.6 kN/mm capable of withstanding the load of 1.65 kN. It is concluded that 50% porous lattice structure has the favourable stiffness of 8.4 kN/mm which makes it as potential for supporting bone fusion with favourable nutrient transport.

Nigel et al. [82] studied the dimensional accuracy and surface finish of three different parts printed using the VW RGD835, High Temp RGD 525 and Clear Biocompatible MED610 materials. Parts were printed with positive (+500 μm) and

Table 4 Summary of the materials and elastic modulus of the polyjet printed parts

Materials	Machine utilized	Variable parameters	Enhancement in properties	Ref
water-soluble SUP707	Objet Eden 260VS	Resolutions (16 and 32 µm)	Improved modulus and strength in high resolution printed specimen	[80]
MED610	Stratasys Objet500 Connex3	Porosity (50% and 70%) and beam diameter (0.4–1.0 mm)	Improved modulus in specimen built with high porosity under large beam diameter	[81]
VW RGD835, High Temp RGD 525 and Clear Bio-compatible MED610	Objet 260 Connex 1	Built direction (X and Y)	Improved surface finish in all specimens	[82]

negative features (-500 µm) in the direction of print head traverse direction and also normal to the traverse direction. Dimensional accuracy of the parts was assessed using a Keyence 3D Digital Microscope (VHX2000E). Roughness measurements were done through WYKO NT1100 white light interferometer from Vecco. Dimensional measurements revealed that negative features are in agreement with the desired depth, whereas the positive features are resulted than the desired height of 500 µm. The deviation in positive features lie around 3–7.5% for all the three printed materials. This is attributed to the viscous behaviour of the photopolymer which caused the partially cured polymer to flow across the surface of the part and consequently resulted in reduction of desired height. Surface roughness of all the three materials was found in the range of approximately 0.2–0.45 µm. It is attributed to the nature of manufacturing process employed irrespective of the materials printed.

Comparison of properties of polyjet printed parts with diverse processed parts

As numerous AM technologies are currently in usage, the choice of the specific process for the specific application is not yet explored in detail. Table 5 summarizes the materials and their improved properties of the polyjet printed parts compared with other additive technologies.

Asuncion Martinez-Garcia et al. [83] investigated the effect of different AM techniques on the mechanical properties of polymer parts for the Safe customized toys. VeroPure, Fullcure and ABS-like materials were produced through polyjet process in Objet Polyjet Stratasys J750. Polyamide 12 material was printed through laser sintering process using Sinterstation 2500plus. PLA part was printed using FDM process in MakerBot FDM Replicator 5th generation. Tensile tests were performed using the UTM (Instron 6025) under the speed of 1 mm/min according to UNE EN ISO 527. Flexural properties of the samples were also measured using UTM with the cross head speed of 2 mm/min according to UNE EN ISO 178. Charpy tests were performed at the velocity of 3.8 m/s and swing angle of 160° using a 1 J hammer. In case of polyjet printing, decreasing layer thickness tends to enhance the mechanical properties such as Young's modulus, tensile strength, flexural strength and impact strength of the parts due to better consolidation, as shown in Fig. 9.

For laser sintered parts, compact structure parts possessed better mechanical properties than honeycomb fill structured. In FDM build parts, horizontal and vertical built parts have better mechanical performance than parts built in 45° orientation. It is reported that laser sintering and FDM process built materials are resistant enough for manufacturing these specific toys, compared to the more fragile polyjet resins.

In addition to the investigation on mechanical properties of parts manufactured through diverse processes, researchers have also explored dimensional accuracy of the parts produced through different additive techniques.

Radomir Mendricky et al. [84] attempted on analysing the accuracy of different additive techniques by means of the selected 3D printers. Printers such as Stratasys Dimension SST 768 printer (FDM principle) and Objet Connex 500 (*PolyJet Matrix)* were used for the experimental purpose. In polyjet printing, *VeroGray*

Table 5 Summary of the materials and properties of the polyjet printed parts compared with diverse processed parts

Materials and machine utilized	Inference	Ref
VeroPure, Fullcure and ABS- Objet Polyjet Stratasys J750 Polyamide 12-Sinterstation 2500plus PLA—MakerBot FDM	Improved strength in FDM and laser sintered specimens than polyjet specimens	[83]
VeroGray RGD850—Objet Connex 500 ABS-P400- Stratasys Dimension SST 768	Accuracy does not lie within the manufacturer specification in both technologies	[84]
VeroGray RGD850—Objet Connex 500 ABS-P400- Stratasys Dimension and Fortus	Accuracy found better in polyjet printed glossy finish parts than FDM parts	[85]
RGD-840—Objet 30 PLA—Ultimaker-2, MakerBot Replector-2	Accuracy was found better in polyjet printed parts, whereas the cost is higher than FDM parts	[86]

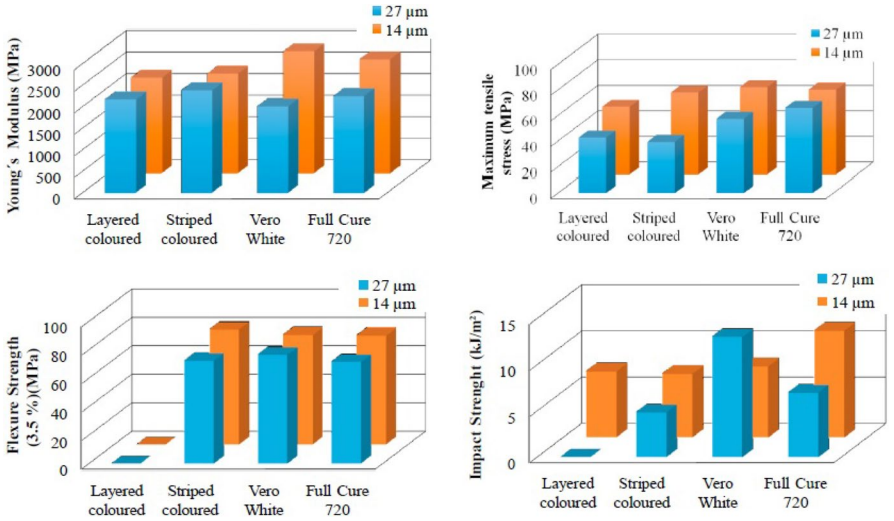

Fig. 9 Variation of mechanical properties of the 3D printed polyjet samples with respect to different layer thickness (with kind permission from Elsevier publisher [83])

RGD850 material was printed under layer thickness of 16 microns (HQ—*High Quality*) and 30 microns (HS—*High Speed*). In FDM process, ABS-P400 was constructed constantly for the layer thickness 250 microns under solid and sparse mode. Digitisation of the printed specimens was performed by GOM *ATOS II 400 3D* contactless scanner equipped with an optic element. This analysis includes the measurement of diameters, length or spacing. Inner and outer diameter measurements were performed and found that deviations of the elements produced through *Stratasys Dimension SST* 768 lie within the tolerances quoted by the printer manufacturer. However, the accuracy of 0.127 mm was exceeded in absolute nominal dimension of vertical Z axis due to the internal tension resulting from material cooling. On the other hand, Objet Connex 500 manufacturer provided the accuracy of the part ranging from 0.02 to 0.085 mm. The value of 0.085 mm was exceeded while printing at high speed setting, i.e. for the layer thickness of 30 µm and this might be due to shrinkage of material.

Same research group [85] addressed the change of properties (dimensional and shape) with respect to time (0, 14 and 84 days) in the samples printed through different techniques. *VeroGray* material was printed under matte and glossy mode through polyjet matrix process, setting the layer thickness as 16 microns (HQ—*High Quality*) and 30 microns (HS—*High Speed*). ABS-P400 material was printed in FDM technology using two different printers such as Dimension and Fortus, with constant layer thickness of 250 microns under sparse and solid mode. Under polyjet printing process, glossy mode gave better results than the matte mode printed parts. After 14 days, polyjet glossy mode had change the dimensions very less (0.04 to 0.05 mm) compared to others. The same performance of polyjet glossy mode printed parts was retained during inspection even after 84 days. In case of FDM technology, dimensional measurements results revealed that FDM Fortus gave better results than the

models from FDM dimension. In dimension printer, printing accuracy of 0.127 mm has been exceeded in vertical Z axis in the range of -0.19 to + 0.16 mm caused by the internal tension resulting from the material cooling.

Similar kind of work [86] was focussed on comparative study of dimensional accuracy of an automotive part (connecting rod) produced through polyjet 3D printing system (Objet 30) and FDM technology (Ultimaker-2, MakerBot Replector-2). In polyjet technology, RGD-840 was used as build material under the thickness of 28 µm. In FDM technology, 0.1 mm thickness was maintained to print the PLA plastic material. Dimensional accuracy of the connecting rod printed through different technology was measured. Results revealed that Objet 30 has minimum percentage error along XY plane (0.99%) than Ultimaker (1.69) and MakerBot (1.63%). In case of radial dimension, Objet 30 has the minimum error (0.53%) than Ultimaker (0.92%) and MakerBot (1.75%). Circular dimension measurement reveals that Objet made part has the least error of 0.74%. In addition, Objet made part has the minimum form error and surface roughness, which is evident that polyjet technology performed well than FDM technology. However, the cost analysis showed that total cost for making the prototype through Objet 30 printer (INR 22,048) was higher than Ultimaker (INR 980) and MakerBot (INR 2134). It is reported that cost aspects should also be considered during production of parts through additive technologies. On the contrary, dimensional accuracy was found as the significant factor rather than cost factor when manufacturing critical component. Hence, it is essential to know the limitations of the quality and accuracy provided by the additive technology.

Mechanical properties of FDM printed parts

In FDM process, mechanical properties of important and potential polymeric materials such as ABS, PLA, PEEK and PEI are studied. In addition, polymer-based composite developed through FDM process is reviewed in this section.

Influence of different parameters on the mechanical properties of the FDM printed parts.

FDM is one of the AM process in which layer-by-layer addition is performed to create complex parts without expensive tooling and material wastage [87]. FDM printed parts gain importance in several sectors such as aerospace and medical industry [88]. Numerous researchers have concentrated on developing high quality and better performance components [89, 90]. The mechanical properties and quality of FDM printed part rely upon various factors such as infill density, infill pattern, layer thickness, print speed, raster angle, nozzle temperature, built direction and layer orientation [91, 92]. However, researches were focussed upon investigating various combinations of the foresaid parameter's influence over the properties of the FDM printed part and such research outcomes are briefly presented in this section. Table 6 summarizes the materials and their improved properties of FDM printed parts under the influence of different parameters.

Table 6 Summary of the materials and properties improvement on FDM parts under the influence of different parameters

Materials	Machine utilized	Variable parameters	Enhancement in properties	Ref
Nylon	Julia Dual	Fill density (50, 75 and 100%), layer height (0.1, 0.2 and 0.3 mm) and print speed (60, 65 and 70 mm/sec)	Improved tensile and impact strength in specimen built under high infill, low layer height and higher print speed	[93]
ULTEM 9085	Fortus 450 mc	layer orientation (0°, +45°/- 45°and 90°) and build direction (flat, edge and upright)	Improved tensile strength in specimen built under 0° layer orientation and edge build direction	[97]

Ramesh et al. [93] manufactured 3D Nylon parts using FDM technology using Taguchi L9 orthogonal array technique to study the properties such as UTS, impact strength, flexural strength and shore D hardness. Different levels of input parameters such as fill density (50, 75 and 100%), layer height (0.1, 0.2 and 0.3 mm) and print speed (60, 65 and 70 mm/sec) were employed. The change in UTS with respect to change in different levels of parameters is shown in Fig. 10.

A maximum tensile strength of 43.5 MPa and an impact strength of 1.746 J are accomplished at 0.1 mm layer height, 100% fill density and 70 mm/s print speed. Absence of pores or gaps between the layers and minimum layer height were identified for contributing higher tensile strength to the parts. The highest flexural strength of 24.02 MPa was achieved in 0.2 mm layer height, 100% fill density and 60 mm/s print speed. This is attributed to maximum fill density with minimum print speed that has deposited uniform layer of 0.1 mm layer height and 100% fill density yielded. The highest hardness of 68 was achieved in 0.3 mm layer height, 100% fill density and 70 mm print speed. The contribution of print speed was identified to be the lowest among all the parameters chosen. All the test results were within the predicted results attained through analysis of variance (ANOVA) at a confidence interval of 95%. It is concluded that this research will provide insights on 3D printing of nylon filament in precision manufacturing industries.

With the advancement of FDM AM process for production of end user products, there is great requirement for newer high-performance materials capable of meeting the requirements of different engineering applications. The high-performance materials possess different mechanical, electrical and thermal properties, making them appropriate for a variety of applications [94]. Among those materials, ULTEM 9085 is a thermoplastic material with superior performance that emerges in recent years. It is noted for its high strength and solvent resistance, making it appealing for applications in aerospace, military and automotive sectors [95, 96]. To employ this material in various industries, it is essential to characterize its mechanical properties and

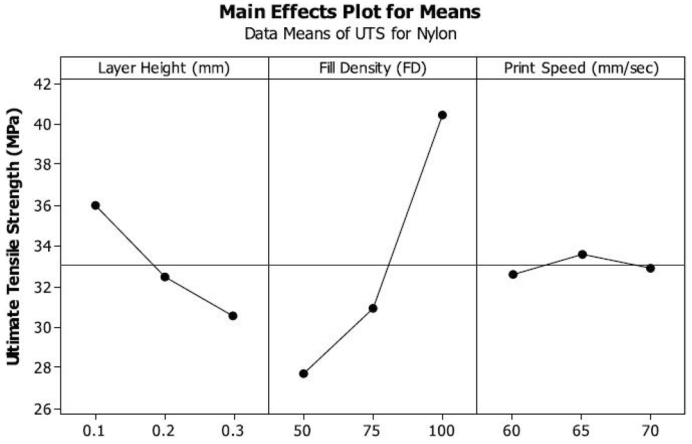

Fig. 10 Main effect plots for UTS with respect change in layer height, fill density and print speed (with kind permission from Elsevier publisher [93])

performance, Hence, Kate Iren Byberga et al. [97] studied the influence of two different process parameters such as layer orientation (0°, + 45°/- 45°and 90°) and build direction (flat, edge and upright) on the mechanical properties of ULTEM 9085 thermoplastic manufactured through FDM process. Layer thickness of 0.254 mm and nozzle diameter of 0.4064 mm were maintained during printing in Fortus 450 mc machine. Tensile specimens were printed according to the ISO standard 527:2012 and the tests were conducted in INSTRON 5985, with a load cell of 250 KN at the speed of 1 mm/min. Average stress–strain curve of ULTEM 9085 thermoplastic material is shown in Fig. 11.

Results reveals that edge printing direction possessed greater strength at all three different layer orientations. Among these, parametric combination of 0° layer orientation and edge build direction shows the highest average UTS of 89 MPa. This is attributed to longer sample width than its thickness in edge building which makes the sample very stronger compared to other building direction. Sample built with parameter combination of 90° layer orientation and edge build direction shows the lowest average tensile strength of 61 MPa due to raster deposition in perpendicular direction to tension load application. It is concluded from this study that mechanical properties of the AM parts are greatly influenced by the process parameters.

Effect of different parameters on the mechanical properties of ABS

ABS is the most widely used thermoplastic printable material for FDM process [98, 99]. Promising properties of ABS such as higher temperature resistance, greater flexibility, better mechanical strength and good machinability all together make it as a good choice for various engineering applications. Hence, several researchers have focussed on studying the effect of process parameters on the properties of ABS printed parts, and the outcomes are briefly presented in this section. Table 7 summarizes the improved properties of ABS under the influence of different parameters

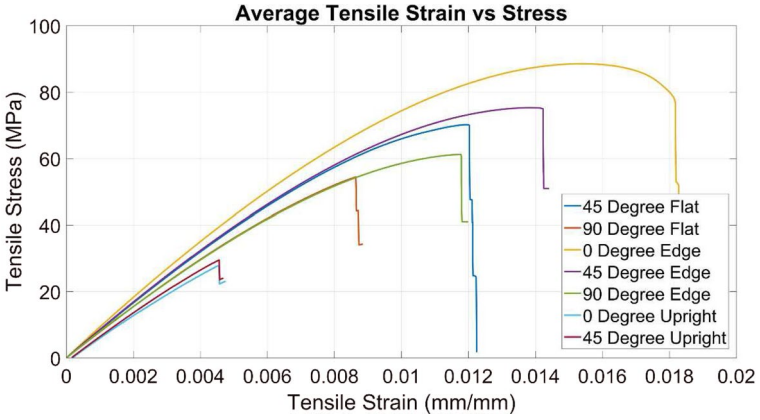

Fig. 11 Average stress–strain curve of ULTEM 9085 thermoplastic material (with kind permission from Elsevier publisher [97])

Table 7 Summary of the properties improvement of ABS under the influence of different parameters

Machine utilized	Variable parameters	Enhancement in properties	Ref
WOL 3D ENDER 3	Infill density (60, 70, 80%), infill pattern (triangle, grid and cubic) and layer thickness (0.1.0.15, 0.2 mm)	Improved tensile strength in specimen built under triangular infill pattern, higher infill and low layer thickness	[100]
uPrint SE Plus	Built direction (X, Y or Z) and deposition angle (0°, 30° or 45°)	Improved tensile strength in specimen built in X direction under low deposition angle of 0°	[102]
Stratasys, Eden Prairie	Built orientation (along the X, Y and Z axis) and raster angle (0°, 30°, 60° and 90°)	Improved tensile strength in specimen built in X axis under 60° raster angle	[103]
Rainstorm Desktop 2D	Layer height (0.35 mm, 0.4 mm and 0.5 mm), raster angle (45°, 55° and 65°) and infill density (40%, 60% and 80%)	Improved tensile strength in specimen built under high infill and raster angle of 65°	[104]
Uprint SE Plus	Infill (low, high and solid) and built orientation (flat, horizontal and vertical)	Improved tensile strength in specimen built in X direction with high infill	[105]

Srinivasan et al. [100] produced ABS parts using FDM technology under the parameters such as infill density (60, 70 and 80%), infill pattern (triangle, grid and cubic) and layer thickness (0.1, 0.15 and 0.2 mm). Design of experiments was carried out using RSM that was analysed using Design Expert Software. Tensile strength was found to be maximum with triangular infill pattern than the grid and cubic pattern. This is due to higher infill density and reduced layer thickness, which is also shown through the surface plot between infill density and layer thickness (Fig. 12).

Desirability-based response optimization techniques were used to optimize the parameters and the desirability result obtained was 0.956. Infill density and layer thickness were identified to be the most significant factor in improving the tensile strength.

The same research group has printed polyethylene terephthalate glycol (PETG) parts using FDM technology [101]. PETG has properties like high strength, low shrinkage and good chemical resistance. Infill density was varied between 20 and 100% with grid type infill pattern, 0.1 mm layer thickness and 45°raster angle in the process. It is reported that tensile strength increases linearly with infill density and 100% infill density yields the highest tensile strength of 32.12 MPa as shown in Fig. 13.

This is due to the existence of air gap between each bead. Surface roughness decrease with increase in infill density and it reveals a minimum value of 2.87 mm for 0.1 mm layer thickness, 100% infill density and grid infill pattern. It is therefore suggested to produce a part with greater infill density where the surface roughness is highly essential.

Sana Abid et al. [102] investigated on the effect of printing parameters on the tensile properties of ABS printed through FDM. Manufacturing direction (X, Y or Z) and the deposition angle (0°, 30° or 45°) were varied using the response surface methodology, and the parts were printed using uPrint SE Plus machine. Diameter

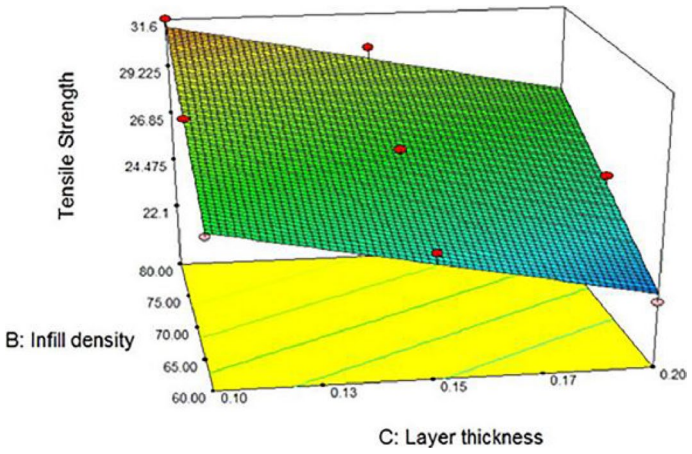

Fig. 12 Surface plot of tensile strength for interaction between infill density and layer thickness (with kind permission from Elsevier publisher [100])

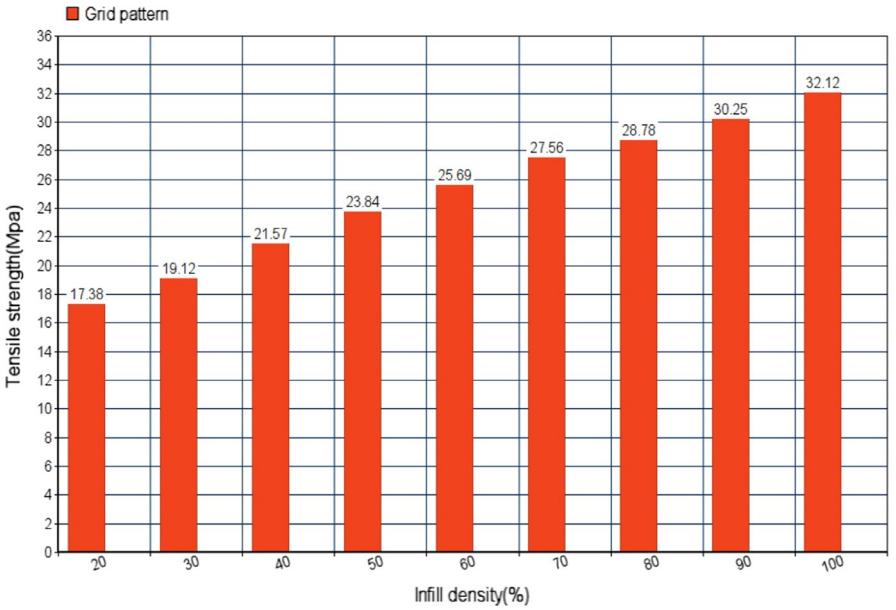

Fig. 13 Plot of tensile strength vs infill density (with kind permission from Elsevier publisher [101])

of the filament was maintained at 1.75 mm; nozzle diameter was set at 254 µm for all the experiments. Tensile tests were performed on the specimen using the UTM (model 8501, Instron, USA) at cross head speeds of 5 mm/s. It is reported that printing orientation has greater significance over the tensile strength compared to that of the deposition angle. It is observed that tensile strength greatly depends on the manufacturing direction (A) and deposition angle (B). Higher tensile strength of 28 MPa resulted for sample built in X direction and low deposition angle of 0° This is attributed to the weakness of filament distortion at low deposition angle and more influence of filament distortion on increasing the deposition angle.

Ashu Garg et al. [103] studied the effect of part building orientation (along the X, Y and Z axis) and raster angle (0°, 30°, 60° and 90°) on the tensile strength of the ABS specimens produced through FDM process. ABS P430 model material was built with the support material according to ASTM D638 standard for tensile testing with the constant thickness of 0.178 mm. Tensile tests were carried out on treated and untreated specimens using Zwick/Roell Z010 UTM equipped with 10 kN load cell and tests were carried at the speed of 5 mm/min. Results reveal that maximum strength is attained in the parts build with X and Y orientation compared to Z orientation. The maximum tensile strength (34.5 MPa) was achieved for a part orientation along the X axis and 60° raster angle (X60), while minimum tensile strength (14.8 MPa) was obtained for a part orientation along the Z axis and 90° raster angle (Z90). This is because the specimens build with a 90° raster angle possess layers aligned in a perpendicular direction to the applied load. This situation tends to cause interlayer cracking, delamination and separation of adjacent layers. On the contrary,

for parts build with a raster angle other than 90°, the layers are aligned in such a manner that offers higher resistance to tensile failure.

Samykano et al. [104] investigated the influence of three process parameters such layer height (0.35 mm, 0.4 mm and 0.5 mm), raster angle (45°, 55° and 65°) and infill density (40%, 60% and 80%) on the mechanical properties of ABS material produced through FDM technology. Specimens were printed using the Rainstorm Desktop 2D Multicolor Printing i3 for carrying out the tensile test according to ASTM D638. Specimen printed with 0.5 mm layer height, 65° raster angle and 80% infill percentage exhibits highest UTS of 32.649 MPa. It is observed that higher infill percentage and 65° raster angle are found to possess greater resistance towards the tensile load. Higher the thickness of the specimen, lower the distortion effect which eventually results in greater strength.

Kyle Raney et al. [105] studied the effect of specimen mesostructure on the monotonic tensile behaviour of ABS parts manufactured by FDM. Parts were fabricated using uPrint SE Plus printer with nozzle diameter of 0.25 microns. Specimens were printed according to the ASTMD638-02a standard with different infill setting and different build orientation such as flat, horizontal and vertical. Testing was performed using Instron testing machine having capacity of 50 tons at the speed of 5 mm/min. Specimens built in X direction exhibit better strength (3313 psi) than the specimen built in Z direction (2533 psi). It is concluded that built orientation has greater effect on strength and relative position of layers with respect to the applied axial load during tensile testing causes the material to respond differently with different build orientation.

Effect of different parameters on the mechanical properties of PLA based printed parts

Shuheng Wang et al. [106] printed PLA materials using FDM technology. The effect of printing angle (0–100°), layer thickness (0.5, 0.15 and 0.2 mm), fill rate (20, 40 and 100%) and nozzle temperature (195–230 °C) on tensile properties and dynamic mechanical properties of FDM printed materials were investigated. The change in tensile strength with respect to change in level of different parameters is shown in Fig. 14.

It is reported that the printing angle less than 45° leads to interlayer tensile fracture and more than 45° leads to intralayer tensile fracture. Deposition of different layer thickness (0.1 mm and 0.2 mm) at a printing angle of 45°conveyed that interlayer failure occurs under tensile load with an increase in the layer thickness. The failed specimens printed with 0.1 mm and 0.2 mm layer thickness were shown in Fig. 15. Increase in fill rate increases the tensile strength, elastic modulus, elongation and dynamic mechanical properties. This is attributed to the decrease in air gap of the material which tightens the bond between the material layers and the filaments, thereby increasing the PLA molecular segment movement resistance. A nozzle temperature setting of 210 °C–215°C is recommended for better static and dynamic mechanical properties. In case of dynamic loading, PLA materials with a printing angle of 90° have more store load potential and the one with 45° have

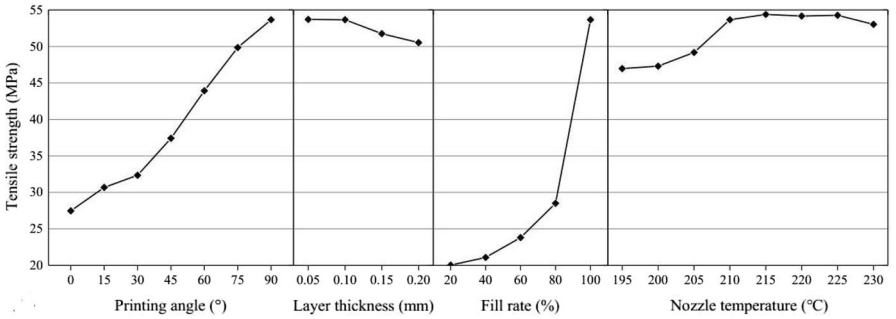

Fig. 14 Variation in tensile strength of PLA with respect to change in printing angle, layer thickness, fill rate and nozzle temperature (with kind permission from Elsevier publisher [106])

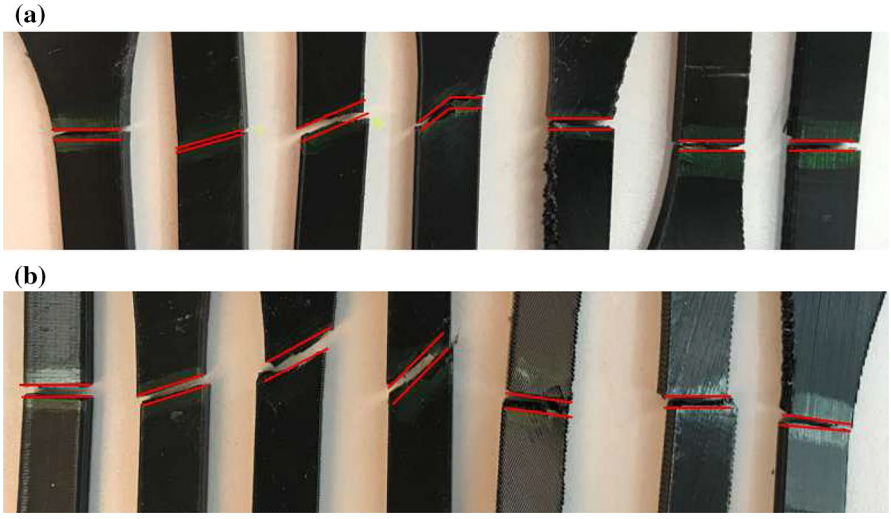

Fig. 15 Fracture characteristics of the specimens a) 0.1 mm and b) 0.2 mm (with kind permission from Elsevier publisher [106])

more potential to dissipate energy rather than storing it. Lesser layer thickness offers greater constraint on the movement of adjacent polymer chains in PLA, leading to a larger loss modulus and loss factor.

Similarly, Qamar Tanveer et al. [107] studied the effect of variable infill density (A = 100%, B = 75%, C = 50%) on the tensile strength of PLA specimens printed by an open-source 3D printer. Specimens were printed with three layers composed of single infill density (AAA, BBB and CCC) and combinations of varying infill density (ABA, BAB, ACA, CAC, BCB, CBC). Tensile specimens were printed according to DIN EN ISO 527–2 and the test is conducted using computerized tensometer KIPLPC 2000 9. It is observed that ABA specimen exhibited the maximum tensile strength of (46.3 N/mm^2), which is slightly higher than specimen A, which is found to be 45.1 N/mm^2. Dense structure was found to give better resistance to

deformation; however, it failed at relatively lower load due to limited flexibility by compact arrangement. The higher tensile strength in ABA specimen is due to varying infill density, i.e. higher density at the outer layers offers resistance towards the crack propagation and inner layers offers greater flexibility before failure.

Faujiya Afrose et al. [108] studied the tensile properties of the PLA processed through FDM process. Parts were printed through Cube-2 3D printer in three different build orientations (X, Y and 45°). Dog-bone-shaped tensile specimens were tested according to ASTM D638 at a strain rate of 50 mm/min using Zwick Z010 testing machine. The specimen build in X, Y and 45° direction possesses the UTS of 38.7 MPa, 31.1 MPa and 33.6 MPa. Highest tensile strength resulted in sample built in X direction and it is attributed to the alignment and bonding parallel to the longer dimension of the specimen. This type of arrangement of layers exhibited maximum resistance towards the deformation in tension than the layers printed in Y and 45° direction. It is concluded that PLA parts produced using smaller FDM machines can also have better mechanical properties and this research provides insights for proper applications of PLA parts using low-cost 3D printers.

Samuel Attoye et al. [109] investigated on the influence of different process parameters such as nozzle temperature (200, 215 and 220 °C), printing speed (20, 40 and 60 mm/s), and print orientation (X, Y and Z) on tensile properties of the PLA and ABS build through FDM process. Tensile properties of the specimens were tested according to the standard ASTM D638 using Q-test machine, Matt Struve Demo MTS Extensometer. It is observed that specimen built in Y orientation exhibited greater mechanical strength (9 ksi) than that of the specimens built over X, Z axis and 45-degree orientation. Higher values of strength are obtained for specimen built at low temperature of 200 °C and highest printing speed of 60 mm/s. It is stated that increasing the built temperature weakens the mechanical properties of the parts.

Uzair Khaleeq uz Zaman et al. [110] studied the impact of FDM process parameters such as layer thickness (0.2 and 0.3 mm), shells (2 and 4), infill pattern (linear and diagonal) and infill percentage (30 and 70%) on the compressive strength of the PLA material. Printing of the samples was done at the speed of 90 mm/s, extruder temperature of 210 °C and heated build surface of 25 °C. Compression tests were conducted for the displacement of 3 mm with the speed of 1 mm/min. It is observed that compression force is influenced by the infill percentage followed by the number of shells, layer thickness and infill pattern. It is concluded that layer thickness of 0.2 mm, number of shells as 4, infill pattern of diagonal and infill percentage (D) of 70%, is observed as the optimum parametric condition to attain optimal compression strength. It is observed that as the shells and infill percentage increases, the compressive strength gets increased due to its lower warping. Diagonal infill pattern performed better than linear pattern as it allows the stresses in the crossed layer to be in indirect tension and shear in a balanced way between the layers thereby withstanding more compressive load.

Jose Camargo et al. [111] studied the effects of layer thickness (0.10 to 0.27 mm) and infill percentage (22 to 89%) on mechanical properties (tensile) in parts manufactured using FDM with PLA graphene. Samples were manufactured using the Delta 3D printer according to ASTM D638-14 standard for tensile testing. Tests were performed using the WDT-20KN with an extensometer at the temperature of

23 ℃ and speed of 5 mm/min. Statistical models were developed to obtain the relationship between the mechanical properties as the function of infill percentage and layer thickness. Tensile strength is significantly influenced by infill percentage and layer thickness according to the model used for analysis. Highest tensile strength of 33.7 MPa was attained for the layer thickness of 0.27 mm and infill of 78%. The maximum value using the model equation was 37.9 MPa with the parameters layer thickness of 0.30 mm and infill of 85%. It is concluded that tensile strength increases with increase in layer thickness and infill percentage. Table 8 summarizes the improved properties of PLA under the influence of different parameters.

Effect of process parameters on the mechanical properties of PEEK and PEI

PEEK and PEI fall under the category of special engineering plastics that possess greater heat resistance and good mechanical properties such as impact and fatigue resistance. The former is a semi-crystalline thermoplastic polymer that has been widely utilized in aerospace, electronics and medicine [112], while the latter is an amorphous thermoplastic polymer that has mostly been used to make high-performance electronic parts and has also served as a biomaterial [113, 114]. Both of them outperform ABS and PLA in terms of heat resistance and mechanical characteristics [115].

Table 9 summarizes the improved properties of PEEK and PEI under the influence of process parameters.

Shouling Ding et al. [116] printed PEEK and PEI parts and studied its mechanical properties under the influence of nozzle temperature and built orientation. The variation in tensile strength of PEEK and PEI parts with increase in nozzle temperature is shown in Fig. 16.

Crystallinity of printed PEEK material offered plasticity and non-crystallinity in printed PEI parts made it brittle. An increase in nozzle temperature from 360 to 420 °C discharges the air pores, thereby improving the density of PEEK and PEI parts. In PEEK samples, printing in horizontal orientation is reported to be stronger than the one printed in vertical orientation. This is due to the superposition direction of the printing layer parallel to the loading direction that absorbs more load. Nevertheless, in case of PEI, the impact strength is low in horizontal orientation which is due to brittle nature. Similarly, Peng Wang et al. [117] evaluated the melting behaviour and fluidity of PEEK in FDM technology using FEA under the influence of different printing parameters. Simulation results recommended an elevated printing head temperature of 380 °C to 440 °C, 4 mm/s wire feeding speed, less than 40 mm/s printing speed and 15 mm length of heating element. Based on the simulated parameters, actual parts were printed using FDM technology. Experimental results concluded that the optimal parameters for printing PEEK are Ø0.4 mm diameter printing head nozzle with a temperature of 440 °C, printing speed of 20 mm/s and printing layer thickness of 0.1 mm. A comparative study was carried out between 3D printed PEEK and injection-moulded PEEK. It is reported that the highest tensile strength of 3D printed PEEK is approximately 80% of the tensile strength of injection-moulded PEEK. This is attributed to higher external pressure of injection

Table 8 Summary of the properties improvement of PLA under the influence of different parameters

Machine utilized	Variable parameters	Enhancement in properties	Ref
Raise3D Pro2 Plus 3D	Printing angle (0–100°), layer thickness (0.5, 0.15 and 0.2 mm), fill rate (20, 40 and 100%) and nozzle temperature (195–230 °C)	Improved elastic modulus, tensile strength and elongation in specimen built with higher infill rate	[106]
Open-source Prusa I3 printer	Infill density (A = 100%, B = 75%, C = 50%)	Improved tensile strength in specimen built under higher infill density	[107]
Cube-2 3D	Build orientations (X, Y and 45°)	Improved tensile strength in specimen built in X direction	[108]
MakerBot	Nozzle temperature (200, 215 and 220 °C), printing speed (20, 40 and 60 mm/s) and print orientation (X, Y and Z)	Improved tensile strength in specimen built in Y direction, low temperature and highest printing speed	[109]
MakerBot replicator	Layer thickness (0.2 and 0.3 mm), shells (2 and 4), infill pattern (linear and diagonal) and infill percentage (30 and 70%)	Improved compressive strength in specimen built under low thickness, high number of shells, diagonal infill and higher infill %	[110]
Delta 3D	Layer thickness (0.10 to 0.27 mm) and infill percentage (22 to 89%)	Improved tensile strength in specimen built under higher layer thickness and infill %	[111]

Table 9 Summary of the properties improvement of PEEK and PEI under the influence of different parameters

Materials	Machine utilized	Variable parameters	Enhancement in properties	Ref
PEEK and PEI	High-temperature 3D	Nozzle temperature (360 °C to 420 °C) and built orientation (vertical and horizontal)	Improved strength in specimen built in horizontal direction under higher nozzle temperature	[116]
PEEK	Ultimaker Cura	Nozzle diameter, temperature, printing speed and layer thickness	Improved tensile strength in specimen build under Ø0.4 mm diameter printing head nozzle with a temperature of 440 °C, printing speed of 20 mm/s and printing layer thickness of 0.1 mm	[117]

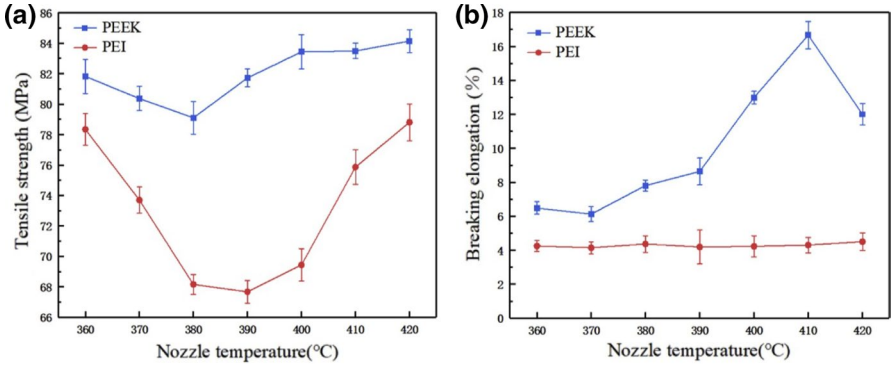

Fig. 16 Variation in tensile strength and elongation of PEEK and PEI parts with respect to change in nozzle temperature (with kind permission from Elsevier publisher [116])

moulding that progresses the density of parts and reduces internal defects. Injection-moulded PEEK yields good fracture toughness compared to the 3D printed PEEK. This is due to the long molecular chains and consequential strong binding forces in injection-moulded PEEK parts. In FDM printed PEEK parts, the polymer chains are rearranged and shortened due to reheating and melting, resulting in inferior fracture toughness. It is concluded that FDM printed PEEK parts can be utilized for the applications wherever better mechanical properties and surface quality are required.

Effect of reinforcement on the mechanical properties of FDM printed composite parts

AM industry is focussed on producing complex geometries with greater flexibility and significant reduction of manufacturing time. In order to improve the performance of monolithic parts, composites are being developed with different reinforcement through FDM process [118, 119]. Table 10 summarizes the materials and reinforcement used for manufacturing of composites and their improved properties.

Elena Verdejo de Toro et al. [120] printed carbon fibre reinforced polyamide parts. The effect on printing parameters like layer height, printing pattern, infill density, nozzle temperature, build plate temperature and printing speed on its mechanical properties was studied. It is reported that the environmental temperature influences the thermal properties of the samples and the degree of crystallinity of materials influences its mechanical properties. Compared to all other parameters, infill density influences more on tensile strength (70–90%) and Young's Modulus (50–60%). 0.8 mm nozzle, 0.2 mm layer height, 100% infill and concentric pattern are reported to be the best combination of parameters to achieve maximum tensile strength, which is also observed through Fig. 17.

In bending test, 100% infill density and 0.2 mm layer height improved the flexural strength to 80–85% and flexural modulus to 55–65%. Likewise, the pattern, the concentric pattern yielded 6–11% higher flexural strength and 22–44% higher flexural modulus than the ± 45 linear pattern. Nozzle diameter offers

Table 10 Summary of the materials and properties of the FDM printed composite parts

Materials	Reinforcement (%)	Machine utilized	Variable parameters	Enhancement in properties	Ref
Polyamide	20 wt %	*Ultimaker 2 Extended+*	Layer height, printing pattern, infill density, nozzle temperature, build plate temperature and printing speed	Improved tensile strength, Young's modulus, flexural strength and flexural modulus bending in the specimen built with 0.8 mm nozzle diameter, 0.2 mm layer height, concentric pattern and 100% infill density	[120]
Multi-wall CNT	1, 3, 5, 7 and 10 wt %	3Dison Pro	Raster pattern (linear and crossed layering)	Improved tensile strength and electrical conductivity in specimen with linear layering	[126]

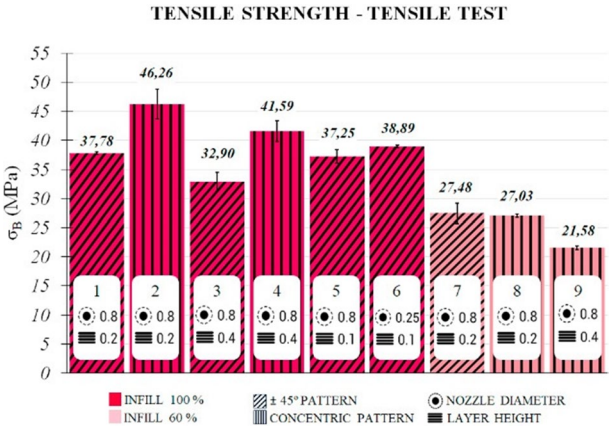

Fig. 17 Variation in tensile strength with respect to nozzle diameter, layer height, infill density and printing pattern (with kind permission from Elsevier publisher [120])

the lowest increase in 5% in flexural strength (5%) and 10% in flexural modulus (10%). The best combination for achieving better results in bending test is 0.25 mm nozzle, 0.1 mm layer height, concentric pattern and an infill density of 100%. Altogether, the best results in mechanical properties are achieved in the combination of 0.8 mm nozzle diameter, 0.2 mm layer height, concentric pattern and 100% infill density.

Other than carbon fibre, especially addition of the carbon nanotubes (CNTs) fillers can potentially improve properties such as electrical/heat conduction, mechanical strength, modulus of elasticity, toughness and durability of 3D printed nano-composites for many potential applications [121–125]. Therefore, Kursad Sezer et al. [126] printed multi-wall CNT (MWCNT) reinforced ABS matrix composite parts using FDM technology with twin-screw micro-compounding extruder and backflow channel facility. Seven wt % MWCNT ABS ratio yielded a maximum tensile strength of 58 MPa (Fig. 18), which can be also seen through the stress–strain diagram (Fig. 19). An overall increase in UTS of 288% was attained when compared to blank ABS. Raster pattern with linear layering [0, 90] resulted in higher UTS than the crossed [–45, 45] layering. This is due to the uniaxial loading along the CNTs in linear layering during the tensile test. In 10 wt% MWCNTs, the electrical conductivity value achieved is highest (232 e^{-2} S/cm), whereas the Melt Flow Index (MFI) value reduces to 0.03 g /10 mm. The variation of electrical conductivity with the MFI value of 10 wt % MWCNT is 164 times less than pure ABS. Decrease in MFI value is due to clogging of nozzle during 3D printing process using filaments with higher MWCNT filler rates. It is concluded that reinforcing carbon/carbon nano-tubes enhances not only the mechanical properties but also the electrical properties of the FDM parts.

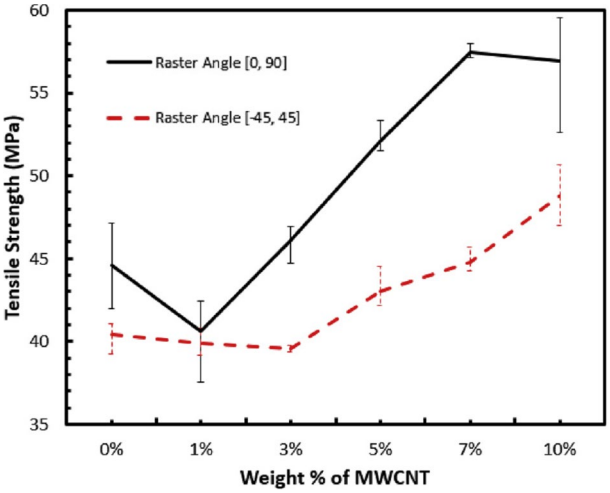

Fig. 18 Variation of tensile strength in 3D printed MWCNTs/ABS composite test specimens with respect to weight % of CNTs (with kind permission from Elsevier publisher [126])

Effect of post-heat treatment on the mechanical properties of FDM printed parts

AM through FDM technique enhances the flexibility and rapidity in production of high strength but lightweight polymeric parts. These polymeric parts have been extensively used in aerospace development and human implants. Among these, PEEK has attractive mechanical properties and environmental resistance over extended temperatures [127–139]. Table 11 summarizes the materials and their improved properties under the influence of heat treatment.

Hence, Yachen Zhao et al. [140] fabricated PEEK structures using FDM technique and studied the effect of raster angle, nozzle temperature and ambient temperature on its mechanical properties. Raster angle of 0°(95, 108 MPa) revealed superior tensile properties when compared to 45° (90, 104 MPa) and 90° (82, 98 MPa) in FDM and extrusion processes, respectively. This is attributed to different degree of interfacial adhesion strengths and fragile connection between filaments as the raster angle gets increases.

It can be observed from Fig. 20 that the nozzle temperature of 400 °C, the ambient temperature of 80 °C and post-heat treatment temperature of 250 °C were identified as optimum parameters to achieve maximum tensile strength of 103 MPa. A physical-based model of cranial implant was fabricated using various nozzle temperatures (380,400,420 °C) parameters without post-treatment/with post-heat treatments (175,200 °C) and subjected to mechanical loading tests. Heat treatment increases the mechanical performance of cranial implant up to a load-bearing capacity of 7000 N.

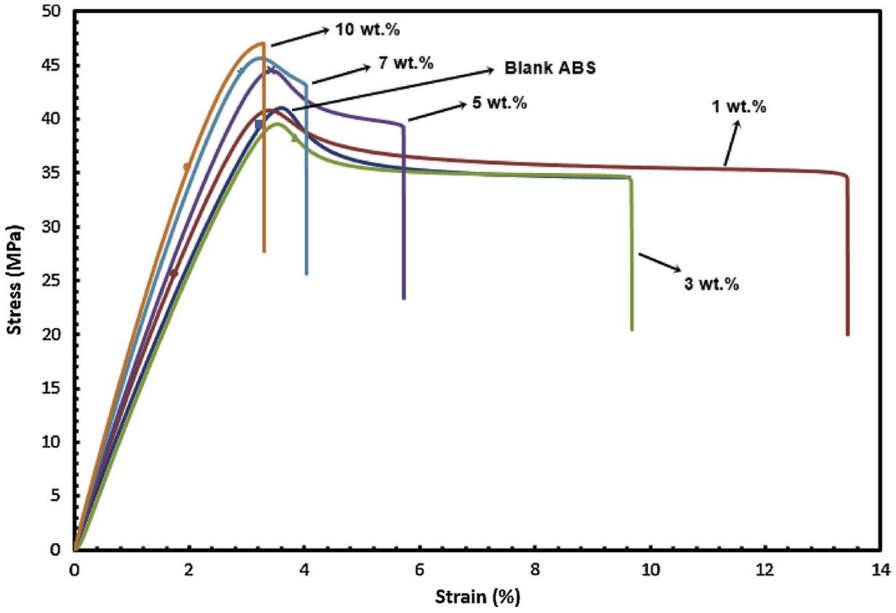

Fig. 19 Stress–strain diagram of MWCNT/ABS and blank ABS tensile test specimen (with kind permission from Elsevier publisher [126])

It is observed that heat-treated cranial implant has broken into fragments before attaining the maximum load for smaller displacement indicating brittle failure. It is concluded that findings of this research work provide guidelines for FDM of PEEK to the clinical implementation and application of cranial implants.

In addition to PEEK, PLA is being extensively manufactured through the FDM technology and exploring about the heat treatment of such parts is highly essential. Setting of heat treatment conditions with respect to several factors is a bigger challenge for the 3D processed parts. An attempt was done to assess the homogeneous heating condition of FDM printed parts for improving the mechanical properties. The heating effect on the parts was studied with respect to layer thickness to establish its influence on the performance of the FDM processed parts. PLA specimens were printed using the 3DISON Plus printer for the layer thickness of 0.1 to 0.3 mm. Tensile strength of the specimen with respect to increase in thickness (0.1, 0.2 and 0.3 mm) was 59.9, 44.0 and 23.5, respectively. Samples built under the higher layer thickness (0.3 mm) were observed with voids, weak adhesion and higher surface roughness, whereas the low layer thickness built samples was not observed with detrimental effects and higher density was observed. This is due to the tight stacking of the rasters in case of lower thickness than the higher layer thickness [141].

In addition to monolithic PLA manufacturing through additive technology, PLA-based composites were also manufactured and subjected to further heat treatment for better mechanical performance. Carbon reinforced PLA was fabricated through FDM technology and the influence of post-processing parameters in its mechanical properties was investigated. PLA was reinforced with 15% of carbon short fibre

Table 11 Summary of the materials and properties of the post-heat-treated FDM printed parts and composites

Materials	Machine utilized	Variable parameters	Post-treatment	Enhancement in properties	Ref
PEEK	In-house developed 3D printer	Raster angle, nozzle temperature and ambient temperature	Heat treatment	Improved tensile strength in specimen built under nozzle temperature of 400 °C,, ambient temperature of 80 °C and post-heat treatment temperature of 250 °C	[140]
PLA	3DISON Plus	Layer thickness (0.1 to 0.3 mm)	Homogeneous heating	Improved strength in specimen built with low layer thickness and heat treated	[141]
PLA-15% carbon fibre	FDM	Layer thickness of 0.2 mm and 90° orientation	Chemical treatment and heat treatment	Improved tensile strength in chemical-treated samples compared to the heat-treated samples	[142]

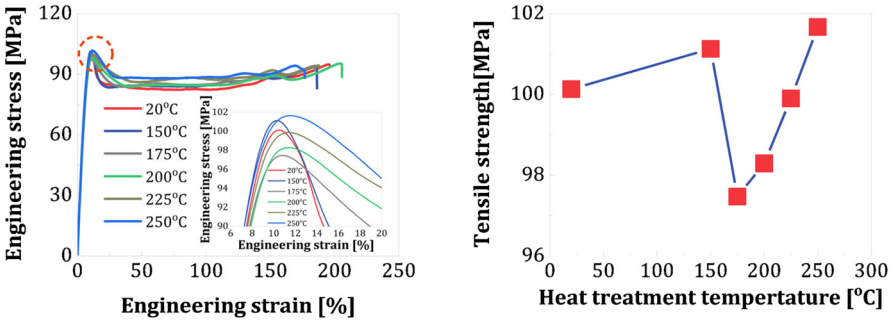

Fig. 20 Stress strain and tensile behaviour of samples under different post-treatment temperatures with the raster angle of 0°, nozzle temperature of 400 °C and ambient temperature of 80 °C (with kind permission from Elsevier publisher [140])

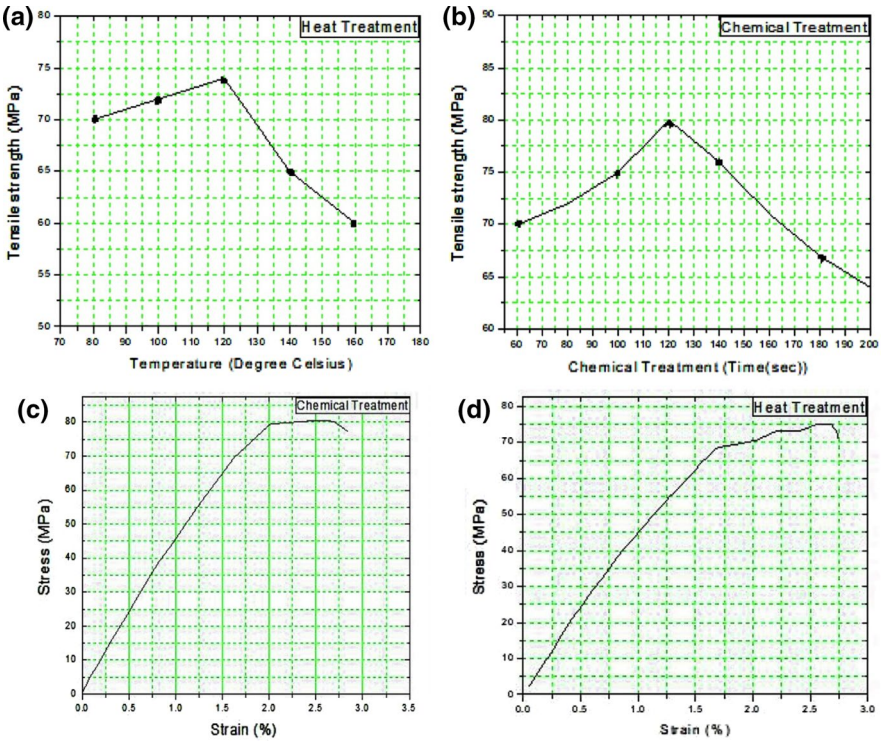

Fig. 21 **a** Tensile strength with respect to temperature with heat treatment process; **b** tensile strength with respect to time in chemical treatment; **c** stress–strain curve of chemical treatment; **d** stress–strain curve of heat treatment (with kind permission from Elsevier publisher [142])

(size of 200 µm and 10 µm diameter) and printed with the layer thickness of 0.2 mm and 90° orientation. Two different post-treatments were applied such as chemical treatment and heat treatment. In case of chemical treatment, samples were soaked in

the acetone solution for different time period ranging from 60 to 220 s. Under heat treatment, samples are heat treated from the temperature range of 80 to 160 °C for time period of 60 to 180 s. Overall, the chemical-treated samples performed better compared to the heat treatment method, which can be inferred from Fig. 21.

Tensile strength of the samples was increased around 12% through the chemical treatment process, whereas only 6% enhancement resulted with the heat treatment process. This is due to the more rearrangement of matrix and fibre in chemical-treated samples than heat-treated samples. Therefore, it is inferred that heat treatment process is lesser effective. Hence, it is suggested to optimize the processing conditions in order to attain the desired mechanical properties through any post-treatment [142]

Effect of different FDM printers on the mechanical properties of FDM printed parts

Cost of the components made from ABS filament material on FDM printer relies on three different parameters such as FDM printer used for printing, brand of filament/support material consumed and time taken for printing the part. One of the prominent methods to reduce the cost is to use low-cost ABS materials and low-cost FDM printer [143]. However, its effect on the mechanical properties has to be analysed. Table 12 summarizes the materials and their improved properties under the influence of different FDM printers.

A comparative study on mechanical properties of components printed using low-, medium- and high-cost FDM printers with different ABS filament material combinations was made by Sunil Khabia et al. [144]. The common parameters maintained in all the combinations were 0.4 mm nozzle diameter, 0.2 mm layer thickness, 100% infill and printing orientation on edge. The maximum tensile strength value (35.7 MPa) was achieved with a combination of Arya UNO + printer, low-cost ABS filament material and concentric infill pattern in Ultimaker Curav3.6 slicing software. The load elongation curve for test specimen printed on Arya UNO + with low-cost ABS filament material is shown in Fig. 22.

It is concluded that selection of the option concentric infill pattern in infill setting of the software enhances the tensile strength of the part. It is understood that knowledgeable operators can make use of the controls available for production of quality and high strength components even from the low-cost FDM printer and ABS material.

Same research group [145] investigated the effect of layer thickness on mechanical properties of FDM printed components in two different FDM printers. It is well known that layer thickness has greater significance on the cost. As the layer thickness was doubled, printing time was reduced to half approximately and in turn the cost as well. Z-ABS part was manufactured in Zortrax M200 LPD printer and low-cost ABS part was produced using Accucraft i250 + FDM printer for different layer thickness ranging from 0.09 to 0.29 mm. No significant variation in tensile strength with respect to layer thickness was observed for the specimens printed with Accucraft i250 + printer using low-cost ABS filament. This might be due to the weaker

Table 12 Summary of the materials and properties of the parts printed using different FDM printers

Materials and Machine utilized	Variable parameters	Enhancement in properties	Ref
Low-cost ABS—Arya UNO + low-cost ABS—Accucraft i250 + Z-ABS—Zortrax M200,	Nozzle diameter (0.4 mm), layer thickness (0.2 mm), infill (100%) and printing orientation on edge	Improved tensile strength in specimen printed using Arya UNO + printer with low-cost ABS filament material having concentric infill pattern	[144]
Z-ABS part—Zortrax M200 LPD Low-cost ABS—Accucraft i250 +	Layer thickness (0.09 to 0.29 mm)	Improved tensile strength in specimen built with low layer thickness using Zortrax M200 LPD printer	[145]
ABS and PLA-MOST, Lulzbot Prusa Mendel, Prusa Mendel and Original Mendel	Pattern orientation, layer height and infill	Improved tensile strength in PLA parts compared to ABS parts in all printers	[151]

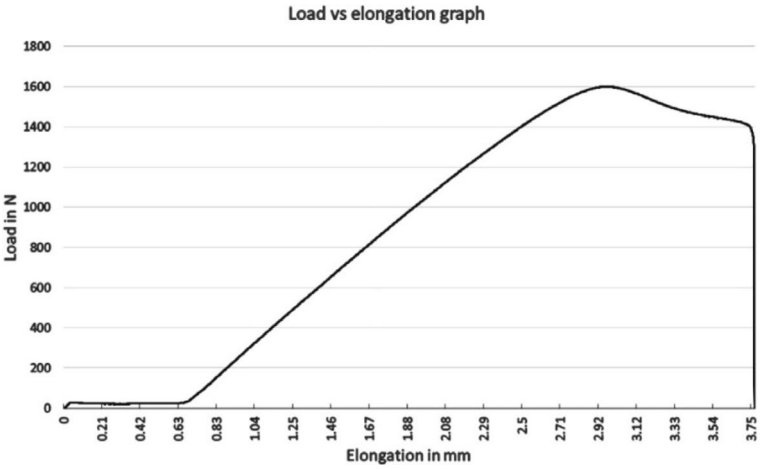

Fig. 22 Load-elongation curve for low-cost ABS filament materials printed on Arya UNO + with kind permission from Elsevier publisher [144]

bonding of the layers even for the infill density of 100%. Specimens printed with the Zortrax M200 LPD printer using Z-ABS filament were observed with greater variation in the tensile strength with respect to change in the thickness. There is an improvement of 20.03% tensile strength from the mean value when the layer thickness is kept low (0.09 mm). The key reason for these phenomena is due to enough strong road to road bonding in infill of a layer. It is concluded that tensile strength of the parts will be higher when the layer thickness is kept low irrespective of the printer and the material but with a variation level in tensile strength.

Along with commercial printers, lot of open-source 3D printers are available under the FDM technology and choice of the printer for the application remains difficult to decide. While OS models have limitations in comparison with industrial methods [146, 147], they are capable of producing very precise components with 0.1 mm positional precision. Moreover, there are open-source 3D printers from RepRap which are available readily to the public at low cost for less than $500 [148]. In such printers, ABS and PLA were primarily manufactured due to its low melting temperatures. Art, toys, tools, home goods and high-value scientific instruments are all made with these machines [149]. Furthermore, RepRaps have been advocated as a tool for small-scale production or as a tool for sustainable development [150].

A study [151] was carried out to quantify the properties of the ABS and PLA made components which enables the users to prefer the 3D printers for manufacturing. Four different printers from RepRap such as MOST, Lulzbot Prusa Mendel, Prusa Mendel and Original Mendel were used for printing the parts. The average tensile strength attained in ABS and PLA was 28.5 MPa and 56.6 MPa, respectively. From these results, it is inferred that 3D printed components from RepRaps printers are found comparable in tensile strength to the parts printed using commercial 3D printing systems. However, importance should be given for the settings, tuning and operation of each individual printer including the type and quality of polymer

filament used. Following these protocols tends to produce stronger parts even with the usage of open-source 3D printers. Therefore, it is concluded that selection of printer for AM should be done in view of balancing the quality, accuracy, properties and cost of manufacturing the parts.

Conclusion

A comprehensive review of mechanical properties of polyjet and FDM printed parts has been carried out. The following conclusions are derived out of the extensive study:

In case of polyjet printing, parts built in X direction are found with superior mechanical properties such as higher tensile strength, bending, compression and hardness than parts printed in Y or Z direction due to higher interfacial strength and presence of cracks/voids in parallel to the direction of application of force. In combined parametric effect, parts built in X direction with glossy finish and with minimal time have greater tensile, flexural, hardness and fatigue properties. Surface finish improvement through glossy finish of the parts improved the fatigue life of the parts. Post-treatment of polyjet parts through UV for more time improved the hardening of the samples and enhances its usage for various applications such as cryogenic conditions, and dental aligners due to its adequate mechanical strength. In overall, mechanical properties of the polyjet printed parts are greatly influenced by the build direction, type of finish and post-processing.

In case of FDM printing, process parameters such as infill density and raster angle have greater significance in controlling the mechanical properties of the parts. Parts with increased infill density (100%) show greater bonding between layers and offer greater resistance to deformation due to decreased air gap between layers. Parts built with raster angle other than 90° offer higher resistance to tensile failure due to absence of filament distortion. Heat treatment increases the load-bearing capacity of samples, especially chemical treatment due to the more rearrangement of matrix and fibre. Overall, infill density and raster angle have to be optimized for attaining better properties in FDM printed parts.

Acknowledgements The authors are grateful to Dr Rajesh Ranganathan, Professor, Coimbatore Institute of Technology for his knowledge sharing in polymer AM for drafting this article.

Authors Contributions PC was involved in review of polyjet printed parts.
RR helped in review of polyjet printed parts FDM.
PD was involved in critical review of polyjet and FDM printed parts.

Declarations

Consent to Publisher Authors have obtained permission for usage of Figs. 1 to 5and7 to 22 from the respective copyright owner/publisher. Figure 6 is taken from the article which is open access; hence, content from this work may be used under the terms of the Creative Commons Attribution 3.0 licence. Any further distribution of this work must maintain attribution to the author(s) and the title of the work, journal citation and DOI. Therefore, the reference of this work has been properly cited in this review work.

References

1. Chapiro M (2016) Current achievements and future outlook for composites in 3D printing. Reinf Plast 60:372–375. https://doi.org/10.1016/j.repl.2016.10.002
2. Leon De, Chen Q, Palaganas N, Palaganas J, Manapat J, Advincula R (2016) High performance polymer nano composites for additive manufacturing applications. React Funct Polym 103:141–155. https://doi.org/10.1016/j.reactfunctpolym.2016.04.010
3. Wang X, Jiang M, Zhou Z, Gou J, Hui D (2017) 3D printing of polymer matrix composites : a review and prospective. Comput Aided Des Compos Part B 110:442–458. https://doi.org/10.1016/j.compositesb.2016.11.034
4. Berman B (2012) 3-D printing: the new industrial revolution. Bus Horiz 55:155–162. https://doi.org/10.1016/j.bushor.2011.11.003
5. Macdonald E, Salas R, Espalin D, Perez M, Aguilera E (2014) 3D printing for the rapid prototyping. IEEE Access 2:234–242. https://doi.org/10.1109/access.2014.2311810
6. Stansbury J, Idacavage M (2016) 3D printing with polymers: challenges among expanding options and opportunities. Dent Mater 32:54–64. https://doi.org/10.1016/j.dental.2015.09.018
7. Mueller B (2012) Additive manufacturing technologies–rapid prototyping to direct digital manufacturing. Assem Autom. https://doi.org/10.1108/aa.2012.03332baa.010
8. Kai CC (1994) Three-dimensional rapid prototyping technologies and key development areas. Comput Control Eng J 5:200–206. https://doi.org/10.1049/cce:19940407
9. Li H, Wang T, Sun J, Yu Z (2018) The effect of process parameters in fused deposition modelling on bonding degree and mechanical properties. Rapid Prototyp J 24:80–92. https://doi.org/10.1108/RPJ-06-2016-0090
10. Sanatgar R, Campagne C, Nierstrasz V (2017) Investigation of the adhesion properties of direct 3D printing of polymers and nano composites on textiles: effect of FDM printing process parameters. Appl Surf Sci 403:551–563. https://doi.org/10.1016/j.apsusc.2017.01.112
11. Melnikova R, Ehrmann AFK (2014) 3D printing of textile-based structures by fused deposition modelling (FDM) with different polymer materials. IOP Conf Series: Mater Sci Eng 62:012018. https://doi.org/10.1088/1757-899X/62/1/012018
12. Melchels F, Feijen J, Grijpma D (2010) A review on stereolithography and itsapplications in biomedical engineering. Biomater 31:6121–6130. https://doi.org/10.1016/j.biomaterials.2010.04.050
13. Ifkovits J, Burdick J (2007) Review: photopolymerizable and degradable biomaterials for tissue engineering. Tissue Eng 13:2369–2385. https://doi.org/10.1089/ten.2007.0093
14. Rengier F, Mehndiratta A, von Tengg-Kobligk H, Zechmann CM, Unterhinninghofen R, Kauczor HU, Giesel FL (2010) 3D printing based on imaging data: review of medical applications. Int J Cars 5:335–341. https://doi.org/10.1007/s11548-010-0476-x
15. Wu G, Hsu S (2015) Review: polymeric-based 3D printing for tissue engineering. J Med Biol Eng 35:285–292. https://doi.org/10.1007/s40846-015-0038-3
16. Morris V, Nimbalkar S, Younesi M, McClellan P, Akkus O (2017) Medicine application, mechanical properties, cytocompatibility and manufacturability of Chitosan: PEGDA hybrid-gel scaffolds by stereolithography. Ann Biomed Eng 45:286–296. https://doi.org/10.1007/s10439-016-1643-1
17. Bakarich S, Gorkin R, Panhuis M, Spinks G (2014) Three-dimensional printing fiber reinforced hydrogel composites. ACS Appl Mater Interf 6:15998–16006. https://doi.org/10.1021/am503878d
18. Kalita S, Bose S, Hosick H, Bandyopadhyay A (2003) Development of controlled porosity polymer-ceramic composite scaffolds via fused deposition modelling. Mater Sci Eng C 23:611–620. https://doi.org/10.1016/S0928-4931(03)00052-3
19. Murphy S, Atala A (2014) 3D bioprinting of tissues and organs. Nat Biotechnol 32:773–785. https://doi.org/10.1038/nbt.2958
20. Crivello J, Reichmanis E (2014) Photopolymer materials and processes for advanced technologies. Chem Mater 26:533–5548. https://doi.org/10.1021/cm402262g
21. Lee J, An J, Chua C (2017) Fundamentals and applications of 3D printing for novel materials. Appl Mater Today 7:120–133. https://doi.org/10.1016/j.apmt.2017.02.004
22. Mohammed J (2016) Applications of 3D printing technologies in oceanography. Method Oceanogr 17:97–117. https://doi.org/10.1016/j.mio.2016.08.001
23. Liu R, Wang Z, Sparks T, Liou F, Newkirk J (2017) Aerospace applications of laser additive manufacturing. Laser Additi Manuf. https://doi.org/10.1016/B978-0-08-100433-3.00013-0

24. Goh G, Agarwala S, Goh G, Dikshit V, Sing S, Yeong W (2017) Additive manufacturing in unmanned aerial vehicles (UAVs): challenges and potential. Aerosp Sci Technol 63:140–151. https://doi.org/10.1016/j.ast.2016.12.019
25. Singh S, Ramakrishna S, Singh R (2017) Material issues in additive manufacturing: a review. J Manuf Process 25:185–200. https://doi.org/10.1016/j.jmapro.2016.11.006
26. Monzon M, Ortega Z, Martinez A, Ortega F (2015) Standardization in additive manufacturing: activities carried out by international organizations and projects. Int J Adv Manuf Technol 76:1111–1121. https://doi.org/10.1007/s00170-014-6334-1
27. Sugavaneswaran M, Arumaikkannu G (2015) Analytical and experimental investigation on elastic modulus of reinforced additive manufactured structure. Mater Des 66:29–36. https://doi.org/10.1016/j.matdes.2014.10.029
28. Bellini A, Güçeri S (2003) Mechanical characterization of parts fabricated using fused deposition modelling. Rap. Prototyp. J. 9:252–264. https://doi.org/10.1108/13552540310489631
29. Ahn SH, Montero M, Odell D, Roundy S, Wright PK (2002) Anisotropic material properties of fused deposition modeling ABS. Rapid Prototyp J 8:248–257. https://doi.org/10.1108/13552540210441166
30. Kęsy A, Kotliński J (2010) Mechanical properties of parts produced by using polymer jetting technology. Arch Civil Mech Engg 10:37–50. https://doi.org/10.1016/S1644-9665(12)60135-6
31. Blanco D, Fernandez P, Noriega A (2014) Nonisotropic experimental characterization of the relaxation modulus for PolyJet manufactured parts. J Mater Res 29:1876–1882. https://doi.org/10.1557/jmr.2014.200
32. Mueller J, Shea K (2015) The effect of build orientation on the mechanical properties in inkjet 3d printing, Solid Freeform Fabrication Symposium, Austin, 983–992.
33. Sugavaneswaran M, Arumaikkannu G (2014) Modelling for randomly oriented multi material additive manufacturing component and its fabrication. Mater Des 54:779–785. https://doi.org/10.1016/j.matdes.2013.08.102
34. Bass L, Meisel NA, Williams CB (2016) Exploring variability of orientation and aging effects in material properties of multi-material jetting parts. Rapid Prototyp J 22:826–834. https://doi.org/10.1108/RPJ-11-2015-0169
35. Es-Said FOS, Noorani J, Mendelson R, Marloth M, Pregger BA (2007) Effect of layer orientation on mechanical properties of rapid prototyped samples. Mater Manufac Process 15:107–122. https://doi.org/10.1080/10426910008912976
36. Majewski C, Hopkinson N (2010) Effect of section thickness and build orientation on tensile properties and material characteristics of laser sintered nylon-12 parts. Rapid Prototyp J 17:176–180. https://doi.org/10.1108/13552541111124743
37. Raut S, Jatti VS, Khedkar NK, Singh TP (2014) Investigation of the effect of build orientation on mechanical properties and total cost of FDM parts. Proced Mater Sci 6:1625–1630. https://doi.org/10.1016/j.mspro.2014.07.146
38. Gajdos I, Spišák E, Slota J, Kaščák Ľ (2013) Influence of path generation strategy on tensile properties of FDM prototypes. Appl Mech Mater 474:273–278. https://doi.org/10.7862/rm.2013.13
39. Qu IV, Bass LB, Williams CB, Dillard DA (2018) Characterizing the effect of print orientation on interface integrity of multimaterial jetting additive manufacturing. Addit Manufac 22:447–461. https://doi.org/10.1016/j.addma.2018.05.036
40. Lumpe TS, Mueller J, Shea K (2019) Tensile properties of multi-material interfaces in 3D printed parts. Mater Des 162:1–9. https://doi.org/10.1016/j.matdes.2018.11.024
41. Rangarajan S, Sunitha K, AnnaMahesh A (2019) Analysis of part built orientation of the polyjet 3 d printed polymer component. Int J Innov Technol Expl Engg. 8(19):3355–3359. https://doi.org/10.35940/ijitee.I8958.078919
42. Das SC, Ranganathan R, Murugan N (2018) Effect of build orientation on the strength and cost of PolyJet 3D printed parts. Rapid Prototyp J 24:832–839. https://doi.org/10.1108/RPJ-08-2016-0137
43. Maroti Peter, Varga Peter, Abraham Hajnalka, Falk Gyorgy, Zsebe Tamas, Meiszterics Zoltan, Mano Sandor, Csernatony Zoltan, Rendeki Szilard, Nyitrai Miklos (2019) Printing orientation defines anisotropic mechanical properties in additive manufacturing of upper limb prosthetics. Mater Res Exp. 6:035403
44. O'Neill P, Jolivet L, Kent NJ, Brabazon D (2017) Physical integrity of 3D printed parts for use as embossing tools. Adv Mater Process Technol 3:308–317. https://doi.org/10.1080/2374068X.2017.1330842

45. Chacón JM, Caminero MA, García-Plaza E, Núñez PJ (2017) Additive manufacturing of PLA structures using fused deposition modelling: effect of process parameters on mechanical properties and their optimal selection. Mater Des 124:143–157
46. Cazon A, Morer P, Matey L (2014) PolyJet technology for product prototyping: tensile strength and surface roughness properties. Proc I Mech E Part B: J Engg Manufac 228:1664–1675. https://doi.org/10.1177/0954405413518515
47. Pugalendhi A, Ranganathan R, Chandrasekaran M (2019) Effect of process parameters on mechanical properties of VeroBlue material and their optimal selection in PolyJet technology. Int J Adv Manuf Technol 108:1049–1059. https://doi.org/10.1007/s00170-019-04782-z
48. Arivazhagan Pugalendhi, Rajesh Ranganathan, Sivakumar Ganesan (2019) Impact of process parameters on mechanical behaviour in multi-material jetting. Mater Today Proceed. https://doi.org/10.1016/j.matpr.2019.12.106
49. Moore J, Williams C (2012) Fatigue characterization of 3D printed elastomer material, in: Solid Freeform Fabrication Proceedings. Annual International Solid Freeform Fabrication Symposium, University of Texas, Austin.
50. Moore JP, Christopher W (2015) Fatigue properties of parts printed by PolyJet material jetting. Rapid Prototyp J 21:675–685. https://doi.org/10.1108/RPJ-03-2014-0031
51. Kumar K, Kumar GS (2015) An experimental and theoretical investigation of surface roughness of poly-jet printed parts. Virt Phys Prototyp 10:23–34. https://doi.org/10.1080/17452759.2014.999218
52. Gay P, Blanco D, Pelayo F, Noriega A, Fernandez P (2015) Analysis of factors influencing the mechanical properties of flat polyjet manufactured parts. Proc Engg 132:70–77. https://doi.org/10.1016/j.proeng.2015.12.481
53. Costa CA, Linzmaier PR, Pasquali FM (2013) Rapid prototyping material degradation: a study of mechanical properties. IFAC Proc 46:350–355. https://doi.org/10.3182/20130911-3-BR-3021.00118
54. Mueller J, Kim S, Shea K, Daraio C (2015) Tensile properties of inkjet 3d printed parts: critical process parameters and their efficient analysis, in: Proceedings of the ASME 2015 International Design Engineering Technical Conferences & Computers and Information in Engineering Conference IDETC/CIE 2015, Boston, Massachusetts, USA.
55. Wang Li, Yang Ju, Xie H, Ma G, Mao L, He K (2017) The mechanical and photoelastic properties of 3D printable stress visualized materials. Scient Rep 7:10918. https://doi.org/10.1038/S41598-017-1143
56. Hong SY, Chan Kim Y, Wang M, Kim H-I, Byun D-Y, Nam J-D, Chou T-W, Ajayan PM, Ci L, Suhr J (2018) Experimental investigation of mechanical properties of UV-Curable 3D printing materials. Polym 145:88–94. https://doi.org/10.1016/j.polymer.2018.04.067
57. Weiss KP, Bagrets N, Lange C, Goldacker W, Wohlgemuth J (2015) Thermal and mechanical properties of selected 3D printed thermoplastics in the cryogenic temperature regime. IOP Conf Series: Mater Sci Engg 102:012022. https://doi.org/10.1088/1757-899X/102/1/012022
58. Levy GN, Schindel R, Kruth JP (2003) Rapid manufacturing and rapid tooling with layer manufacturing (LM) technologies, state of the art and future perspectives. CIRP Ann 52:589–609. https://doi.org/10.1016/S0007-8506(07)60206-6
59. Yan X, Gu P (1996) A review of rapid prototyping technologies and systems. Comput Des 28:307–318. https://doi.org/10.1016/0010-4485(95)00035-6
60. Birkeland K, Katle A, Løvgreen S, Bøe OE, Wisth PJ (1999) Factors influencing the decision about orthodontic treatment. A longitudinal study among 11- and 15-year-olds and their parents. J Orofac Orthop 60:292–307. https://doi.org/10.1007/BF01301243
61. Hazeveld A, Huddleston Slater JJR, Ren Y (2014) Accuracy and reproducibility of dental replica models reconstructed by different rapid prototyping techniques. Am J Orthod Dentofacial Orthop 145:108–115. https://doi.org/10.1016/j.ajodo.2013.05.011
62. El-Katatny I, Masood SH, Morsi YS (2010) Error analysis of FDM fabricated medical replicas. Rapid Prototyp J 16:36–43. https://doi.org/10.1108/13552541011011695
63. Lee KY, Cho JW, Chang NY, Chae JM, Kang KH, Kim SC (2015) Accuracy of three-dimensional printing for manufacturing replica teeth. Korean J Orthod 45:217–225. https://doi.org/10.4041/kjod.2015.45.5.217
64. Bajaj D, Madhav I, Juneja M, Tuli R, Jindal P (2018) Methodology for stress measurement by transparent dental aligners using strain gauge. World J Dent. https://doi.org/10.5005/jp-journals-10015-1499

65. Ahn HW, KimK A, Kim SH (2015) A new type of clear orthodontic retainer incorporating multi-layer hybrid materials. Korean J Orthod 45:268–272. https://doi.org/10.4041/kjod.2015.45.5.268
66. Johal A, Sharma NR, McLaughlin K, Zou LF (2015) The reliability of thermoform retainers: A laboratory-based comparative study. Eur J Orthod 37:503507. https://doi.org/10.1093/ejo/cju075
67. Lombardo L, Martines E, Mazzanti V, Arreghini A, Mollica F, Siciliani G (2017) Stress relaxation properties of four orthodontic aligner materials: a 24-hour in vitro study. Angle Orthod 87:11–18. https://doi.org/10.2319/113015-813.1
68. Kohda N, Iijima M, Muguruma T, Brantley WA, Ahluwalia KS, Mizoguchi I (2013) Effects of mechanical properties of thermoplastic materials on the initial force of thermoplastic appliances. Angle Orthod 83:476–483. https://doi.org/10.2319/052512-432.1
69. Jindal P, Juneja M, Siena FL, Bajaj D, Breedon P (2019) Mechanical and geometric properties of thermoformed and 3D printed clear dental aligners. Amer J Orthod Dentof Orthop 156:694–701. https://doi.org/10.1016/j.ajodo.2019.05.012
70. Singh S, Ramakrishna S (2017) Biomedical applications of additive manufacturing: Present and future. Current Opinion Biomed Eng 2:105–115. https://doi.org/10.1016/j.cobme.2017.05.006
71. Podshivalov L, Gomes CM, Zocca A, Guenster J, Bar-Yoseph P, Fischer A (2013) Design, analysis and additive manufacturing of porous structures for biocompatible micro-scale scaffolds. Proced CIRP 5:247–252. https://doi.org/10.1016/j.procir.2013.01.049
72. Velasco MA, Lancheros Y, Garzón-Alvarado DA (2016) Geometric and mechanical properties evaluation of scaffolds for bone tissue applications designing by a reaction-diffusion models and manufactured with a material jetting system. J Comput Des Eng 3:385–397. https://doi.org/10.1016/j.jcde.2016.06.006
73. Velasco MA, Narváez-Tovar CA, Garzón-Alvarado DA (2015) Design, materials, and mechanobiology of biodegradable scaffolds for bone tissue engineering. Biomed Res Int 2015:1–21. https://doi.org/10.1016/j.jcde.2016.06.006
74. Butscher A, Bohner M, Roth C, Ernstberger A, Heuberger R, Doebelin N, Rudolf von Rohr P, Müller R (2012) Printability of calcium phosphate powders for three-dimensional printing of tissue engineering scaffolds. Acta Biomater 8:373–385. https://doi.org/10.1016/j.actbio.2011.08.027
75. Suwanprateeb J, Sanngam R, Panyathanmaporn T (2010) Influence of raw powder preparation routes on properties of hydroxyapatite fabricated by 3D printing technique. Mater Sci Eng C 30:610–617. https://doi.org/10.1016/j.msec.2010.02.014
76. Leong K, Cheah C, Chua C (2003) Solid freeform fabrication of three dimensional scaffolds for engineering replacement tissues and organs. Biomater 24:2363–2378. https://doi.org/10.1016/S0142-9612(03)00030-9
77. Gomez S, Vlad M, López J, Fernández E (2016) Design and properties of 3D scaffolds for bone tissue engineering. Acta Biomater 42:341–350. https://doi.org/10.1016/j.actbio.2016.06.032
78. Bibb R, Thompson D, Winder J (2011) Computed tomography characterisation of additive manufacturing materials. Med Eng Phys 33:590–596. https://doi.org/10.1016/j.medengphy.2010.12.015
79. Brunelli M, Perrault C, Lacroix D (2017) Mechanical response of 3D insert® PCL to compression. J Mech Behav Biomed Mater 65:478–489. https://doi.org/10.1016/j.jmbbm.2016.08.038
80. Amini M, Reisinger A, Pahr DH (2019) Influence of processing parameters on mechanical properties of a 3D-printed trabecular bone microstructure. J Biomed Mater Res Part B. 108:38–47. https://doi.org/10.1002/jbm.b.34363
81. Egan PF, Bauer I, Shea K, Ferguson SJ (2019) Mechanics of three- dimensional printed lattices for biomedical devices. J Mech Des 141:031703. https://doi.org/10.1115/1.4042213
82. Kent NJ, Jolivet L, O'Neill P, Brabazon D (2017) An evaluation of components manufactured from a range of materials, fabricated using PolyJet technology. Adv Mater Process Technol 3:318–329. https://doi.org/10.1080/2374068X.2017.1330856
83. Martínez-García A, Sandoval-Pérez I, Ibáñez-García A, Peco K, Varela-Gandía FJ, Galvañ-Gisbert J (2019) Influence of process parameters of different additive manufacturing techniques on mechanical properties and safety of customised toys. Proc Manufac 41:106–113
84. Radomir Mendricky (2016) Accuracy analysis of additive technique for parts manufacturing. Mm Sci J. 1502-1508. https://doi.org/10.17973/Mmsj.2016_11_2016169
85. Phaneendra Mantada, Radomir Mendricky, Jiri Safka (2017) Parameters influencing the precision of various 3d printing technologies. Mm Sci J. 2004–2012 https://doi.org/10.17973/Mmsj.2017_12_201776

86. Maurya Nagendra Kumar, Rastogi Vikas, Singh Pushpendra (2019) Comparative study and measurement of form errors for the component printed by FDM and polyjet process. Instrum Mesur Métrol. 18:353–358. https://doi.org/10.18280/i2m.180404
87. Popescu D, Zapciu A, Amza C, Baciu F, Marinescu R (2018) FDM process parameters influence over the mechanical properties of polymer specimens: a review. Polym Test 69:157–166. https://doi.org/10.1016/j.polymertesting.2018.05.020
88. Jain P, Kuthe AM (2013) Feasibility study of manufacturing using rapid prototyping: FDM approach. Proc Eng 63:4–11. https://doi.org/10.1016/j.proeng.2013.08.275
89. Karapatis NP, Van Griethuysen JPS, Glardon R (1998) Direct rapid tooling: a review of current research. Rap Prototyp J 4:77–89. https://doi.org/10.1108/13552549810210248
90. J Zhou D Herscovici C Calvin Che. 2000. Parametric process optimization to improve the accuracy of rapid prototyped stereolithography parts. Int J Mach Tools Manuf. 40 363 379. https://doi.org/10.1016/S0890-6955(99)00068-1
91. Anitha R, Arunachalam S, Radhakrishnan P (2001) Critical parameters influencing the quality of prototypes in fused deposition modelling. J Mater Process Technol 118:385–388. https://doi.org/10.1016/S0924-0136(01)00980-3
92. Sood AK, Chaturvedi V, Datta S, Mahapatra SS (2011) Optimization of process parameter infused deposition modelling using weighted principle component analysis. J Adv Manuf Syst 2:241–250. https://doi.org/10.1142/S0219686711002181
93. Ramesh M, Panneerselvam K (2020) Mechanical investigation and optimization of parameter selection for Nylon material processed by FDM. Mater Today: Proceed https://doi.org/10.1016/j.matpr.2020.02.697
94. Motaparti K P, Taylor G, Leu M C, Chandrashekhara K, Castle J, Matlack M (2016) Effects of build parameters on compression properties for ULTEM 9085 parts by fused deposition modeling. In: Proceedings of the 27th Annual International Solid Freeform Fabrication Symposium, Austin, TX, USA. 964–977.
95. Bagsik A, Schöppner V, Klemp E (2010) FDM part quality manufactured with Ultem 9085. In: Proceedings of the 14th International Scientific Conference on Polymeric Materials, Halle (Saale), Germany, 15: 307–315
96. Bagsik A, Schöppner V (2011) Mechanical properties of fused deposition modeling parts manufactured with ultem 9085. In: Proceedings of the Society of Plastics Engineers ANTEC Conference (Anaheim), Boston, MA, USA. 1–5.
97. Byberg KI, Gebisa AW, Lemu HG (2018) Mechanical properties of ULTEM 9085 material processed by fused deposition modelling. Polym Test 72:335–347. https://doi.org/10.1016/j.polymertesting.2018.10.040
98. Hwang S, Reyes EI, Moon KS, Rumpf RC, Kim NS (2015) Thermo-mechanical characterization of metal/polymer composite filaments and printing parameter study for fused deposition modelling in the 3D printing process. J Electron Mater 44:7717777. https://doi.org/10.1007/s11664-014-3425-6
99. Wu W, Geng P, Li G, Zhao D, Zhang H, Zhao J (2015) Influence of layer thickness and raster angle on the mechanical properties of 3D printed PEEK and a comparative mechanical study between PEEK and ABS. Mater 8:5834–5846. https://doi.org/10.3390/ma8095271
100. Srinivasan R, Pridhar T, Ramprasath LS, Sree Charan N, Ruban W (2020) Prediction of tensile strength in FDM printed ABS parts using response surface methodology. Mater Today: Proceed 27:1827–1832. https://doi.org/10.1016/j.matpr.2020.03.788
101. Srinivasan R, Ruban W, Deepanraj A, Bhuvanesh R, Bhuvanesh T (2020) Effect on infill density on mechanical properties of PETG part fabricated by fused deposition modeling. Mater Today: Proceed 27:1838–1842. https://doi.org/10.1016/j.matpr.2020.03.797
102. Abid S, Messadi R, Hassine T (2019) Optimization of mechanical properties of printed acrylonitrile butadiene styrene using RSM design. Int J Adv Manuf Technol 100:1363–1372. https://doi.org/10.1007/s00170-018-2710-6
103. Garg A, Bhattacharya A, Batish A (2016) Chemical vapor treatment of ABS parts built by FDM: Analysis of surface finish and mechanical strength. Int J Adv Manuf Technol 89:2175–2191. https://doi.org/10.1007/s00170-016-9257-1
104. Samykano M, Selvamani SK, Kadirgama K, Ngui WK, Kanagaraj G, Sudhakar K (2019) Mechanical property of FDM printed ABS: influence of printing parameters. Int J Adv Manuf Technol 102:2779–2796. https://doi.org/10.1007/s00170-019-03313-0

105. Raneya K, Lanib E, Kallac DK (2017) Experimental characterization of the tensile strength of ABS parts manufactured by fused deposition modeling process. Mater Today: Proceed 4:7956–7961. https://doi.org/10.1016/j.matpr.2017.07.132
106. Wang S, Ma Y, Deng Z, Zhang S, Cai J (2020) Effects of fused deposition modeling process parameters on tensile, dynamic mechanical properties of 3D printed polylactic acid materials. Polym Test 86:106483. https://doi.org/10.1016/j.polymertesting.2020.106483
107. Tanveer MQ, Haleem A, Suhaib M (2019) Effect of variable infill density on mechanical behaviour of 3-D printed PLA specimen: an experimental investigation. SN Appl Sci 1:1701. https://doi.org/10.1007/s42452-019-1744-1
108. Afrose F, Masood SH, Nikzad M, Iovenitti P (2014) Effects of build orientations on tensile properties of PLA material processed by FDM. Adv Mater Res 1044:31
109. Attoye S, Malekipour E, El-Mounayri H (2019) Correlation between process parameters and mechanical properties in parts printed by the fused deposition modeling process. In: Kramer S., Jordan J., Jin H., Carroll J., Beese A. (eds) Mechanics of Additive and Advanced Manufacturing, 8 https://doi.org/10.1007/978-3-319-95083-9_8
110. U Khaleeq uz Zaman, Emilien Boesch, Ali Siadat, Mickael Rivette, Aamer Ahmed Baqai. 2018. Impact of fused deposition modeling (FDM) process parameters on strength of built parts using Taguchi's design of experiments. Int J Adv Manuf Technol. 101 1215 1226. https://doi.org/10.1007/s00170-018-3014-6
111. Camargo JC, Machado AR, Almeida EC, Silva EFMS (2019) Mechanical properties of PLA-graphene filament for FDM 3D Printing. Int J Adv Manuf Technol 103:2423–2443. https://doi.org/10.1007/s00170-019-03532-5
112. Garcia-Gonzalez D, Rusinek A, Jankowiak T, Arias A, Mechanical impact behavior of polyether–ether–ketone (PEEK). Compos Struct 124:88–99. https://doi.org/10.1016/j.compstruct.2014.12.061
113. H Wu M Krifa Ko. 2018. Rubber (SEBS-g-MA) toughened flame retardant polyamide 6: microstructure, combustion, extension, and izod impact behaviour. Polym Plast Technol. 57 727 739. https://doi.org/10.1080/03602559.2017
114. Peluso G, Petillo O, Ambrosio L, Nicolais L (1994) Polyetherimide as biomaterial: preliminary in vitro and in vivo biocompatibility testing. J Mater Sci Mater Med 5:738–742. https://doi.org/10.1007/BF00120367
115. Jenkins MJ (2001) Crystallisation in miscible blends of PEEK and PEI. Polym 42:1981–1986. https://doi.org/10.1016/S0032-3861(00)00438-9
116. Ding S, Zou B, Wang P, Ding H (2019) Effects of nozzle temperature and building orientation on mechanical properties and microstructure of PEEK and PEI printed by 3D-FDM. Polym Test 78:105948. https://doi.org/10.1016/j.polymertesting.2019.105948
117. Wang P, Zou B, Xiao H, Ding S, Huang C (2019) Effects of printing parameters of fused deposition modeling on mechanical properties, surface quality, and microstructure of PEEK. J Mater Process Tech 271:62–74. https://doi.org/10.1016/j.jmatprotec.2019.03.016
118. Parandoush P, Lin D (2017) A review on additive manufacturing of polymer-fiber composites. Compos Struct 182:36–53. https://doi.org/10.1016/j.compstruct.2017.08.088
119. Blok LG, Longana ML, Yu H, Woods BKS (2018) An investigation into 3D printing of fibre reinforced thermoplastic composites. Addit Manufac 22:176–186. https://doi.org/10.1016/j.addma.2018.04.039
120. Verdejo E, de Toro J, Sobrino C, Martinez AM, Eguia VM (2019) Analysis of the influence of variables of the Fused Deposition Modeling (FDM) process on the mechanical properties of a carbon fiber-reinforced polyamide. Proced Manufac 41:731–738. https://doi.org/10.1016/j.promfg.2019.09.064
121. Tekinalp HL, Kunc V, Velez-Garcia GM, Duty CE, Love LJ, Naskar AK (2014) Highly oriented carbon fiber-polymer composites via additive manufacturing. Compos Sci Technol 105:144–150. https://doi.org/10.1016/j.compscitech.2014.10.009
122. Shofner ML, Lozano K, Rodríguez-Macías FJ, Barrera EV (2003) Nanofiber reinforced polymers prepared by fused deposition modeling. J Appl Polym Sci 89:3081–3090. https://doi.org/10.1002/app.12496
123. Leigh SJ, Bradley RJ, Purssell CP, Billson D, Hutchins DA (2012) A simple, low-cost conductive composite material for 3D printing of electronic sensors. PLoS ONE 7:1–7. https://doi.org/10.1371/journal.pone.0049365

124. Postiglione G, Natale G, Griffini G, Levi M, Turri S (2015) Conductive 3D microstructures by direct 3D printing of polymer/carbon nanotube nanocomposites via liquid deposition modeling. Compos Part A Appl Sci Manuf 76:110–114. https://doi.org/10.1016/j.compositesa.2015.05.014
125. Gnanasekarana K, Heijmansa T, van Bennekomb S, Woldhuisb H, Wijniab S (2017) 3D printing of CNT- and graphene-based conductive polymer nanocomposites by fused deposition modeling. Appl Mater Today 9:21–28. https://doi.org/10.1016/j.apmt.2017.04.003
126. Kursad Sezer H, Eren O (2019) FDM 3D printing of MWCNT reinforced ABS nano-composite parts with enhanced mechanical and electrical properties. J Manufac Process 37:339–347. https://doi.org/10.1016/j.jmapro.2018.12.004
127. Berretta S, Davies R, Shyng YT, Wang Y, Ghita O (2017) Fused deposition modelling of high temperature polymers: exploring CNT PEEK composites. Polym Test 63:251–262. https://doi.org/10.1016/j.polymertesting.2017.08.024
128. McLauchlin AR, Ghita OR, Savage L (2014) Studies on the reprocessability of poly(ether ether ketone) (PEEK). J Mater Process Tech 214:75–80. https://doi.org/10.1016/j.jmatprotec.2013.07.010
129. Tseng JW, Liu CY, Yen YK, Belkner J, Bremicker T, Liu BH (2018) Screw extrusion based additive manufacturing of PEEK. Mater Des 140:209–221. https://doi.org/10.1016/j.matdes.2017.11.032
130. Arif MF, Kumar S, Varadarajan KM, Cantwell WJ (2018) Performance of biocompatible PEEK processed by fused deposition additive manufacturing. Mater Des 146:249–259. https://doi.org/10.1016/j.matdes.2018.03.015
131. Rinaldi M, Ghidini T, Cecchini F, Brandao A, Nanni F (2018) Additive layer manufacturing of poly (ether ether ketone) via FDM. Compos Part B-Eng 145:162–172. https://doi.org/10.1016/j.compositesb.2018.03.029
132. Geng P, Zhao J, Wu WZ, Ye WL, Wang YL, Wang SB (2019) Effects of extrusion speed and printing speed on the 3D printing stability of extruded PEEK filament. J Manuf Process 37:266–273. https://doi.org/10.1016/j.jmapro.2018.11.023
133. Yang C, Tian X, Li D, Cao Y, Zhao F, Shi C (2017) Influence of thermal processing conditions in 3D printing on the crystallinity and mechanical properties of PEEK material. J Mater Process Tech 248:1–7. https://doi.org/10.1016/j.jmatprotec.2017.04.027
134. Chien MC, Weiss RA (1988) Strain-induced crystallization behavior of poly(Ether ether ketone) (PEEK). Polym Eng Sci 28:6–12. https://doi.org/10.1002/pen.760280103
135. Nazari B, Rhoades AM, Schaake RP, Colby RH (2016) Flow-induced crystallization of PEEK: isothermal crystallization kinetics and lifetime of flow-induced precursors during isothermal annealing. ACS Macro Lett 5:849–853. https://doi.org/10.1021/acsmacrolett.6b00326
136. Pascual A, Toma M, Tsotra P, Grob MC (2019) On the stability of PEEK for short processing cycles at high temperatures and oxygen-containing atmosphere. Polym Degrad Stab 165:161–169. https://doi.org/10.1016/j.polymdegradstab.2019.04.025
137. Jin L, Ball J, Bremner T, Sue HJ (2014) Crystallization behavior and morphological characterization of poly(ether ether ketone). Polym 55:5255–5265. https://doi.org/10.1016/j.polymer.2014.08.045
138. Rae PJ, Brown EN, Orler EB (2007) The mechanical properties of poly(ether-ether-ketone) (PEEK) with emphasis on the large compressive strain response. Polym 48:598–615. https://doi.org/10.1016/j.polymer.2006.11.032
139. El Halabi F, Rodriguez JF, Rebolledo L, Hurtos E, Doblare M (2011) Mechanical characterization and numerical simulation of polyether-ether-ketone (PEEK) cranial implants. J Mech Behav Biomed Mater 4:1819–1832. https://doi.org/10.1016/j.jmbbm.2011.05.039
140. Zhao Y, Zhao K, Li Y, Chen F (2020) Mechanical characterization of biocompatible PEEK by FDM. J Manufac Process 56:28–42. https://doi.org/10.1016/j.jmapro.2020.04.063
141. Wonjin Jo, O-Chang Kwon, Myoung-Woon Moon, 2018 Investigation of influence of heat treatment on mechanical strength of FDM Printed 3d Objects. Rapid Prototyp J. 24 637 644. https://doi.org/10.1108/rpj-06-2017-0131
142. Guduru S (2020) Effect of post treatment on tensile properties of carbon reinforced PLA composite by 3d printing. Mater Today: Proceed 33:5403–5407. https://doi.org/10.1016/j.matpr.2020.03.128
143. Szykiedans K, Credo W (2016) Mechanical properties of FDM and SLA low-cost 3-D prints. Procedia Eng 136:257–262. https://doi.org/10.1016/j.proeng.2016.01.207

144. Khabia S, Jain KK (2020) Comparison of mechanical properties of components 3D printed from different brand ABS filament on different FDM printers. Mater Today: Proceed 26:2907–2914. https://doi.org/10.1016/j.matpr.2020.02.600
145. Khabia S, Jain KK (2020) Influence of change in layer thickness on mechanical properties of components 3d printed on Zortrax M 200 FDM printer with Z-ABS filament material & Accucraft i250+ FDM printer with low cost ABS filament material. Mater Today: Proceed 26:1315–1322. https://doi.org/10.1016/j.matpr.2020.02.268
146. Kumar S, Kruth JP (2010) Composites by rapid prototyping technology. Mater Des 31:850–856. https://doi.org/10.1016/j.matdes.2009.07.045
147. Horii T, Kirihara S, Miyamoto Y (2009) Freeform fabrication of superalloy objects by 3D micro welding. Mater Des 30:1093–1097. https://doi.org/10.1016/j.matdes.2008.06.033
148. Jones R, Haufe P, Sells E, Iravani P, Olliver V, Palmer C (2011) RepRap – the replicating rapid prototyper. Robot 29:177–191. https://doi.org/10.1017/S026357471000069X
149. Pearce JM (2012) Building research equipment with free, Open-Source Hardware. Sci 337:1303–1304. https://doi.org/10.1126/science.1228183
150. Pearce JM, Morris Blair C, Laciak KJ, Andrews R, Nosrat A, Zelenika-Zovko I (2010) 3-D Printing of open source appropriate technologies for self-directed sustainable development. J Sustain Dev 3:17–29. https://doi.org/10.5539/jsd.v3n4p17
151. K Tymrak Pearce. 2014. Mechanical properties of components fabricated with open-source 3-d printers under realistic environmental conditions Mater Des. 58 242 246. https://doi.org/10.1016/j.matdes.2014.02.038